PERGAMON

Neuropharmacology 37 (1998) 633–655

NEURO PHARMACOLOGY

Hebbian-like functional plasticity in the auditory cortex of the behaving monkey

Ehud Ahissar [a,*], Moshe Abeles [b], Merav Ahissar [c], Sebastian Haidarliu [a], Eilon Vaadia [b]

[a] *Department of Neurobiology, The Weizmann Institute of Science, Rehovot 76100, Israel*
[b] *Department of Physiology, The Hebrew University Hadassah Medical School, Jerusalem 91010, Israel*
[c] *Department of Psychology, The Hebrew University, Jerusalem 91905, Israel*

Accepted 2 April 1998

Abstract

In this study, the necessary conditions, including those related to behavior, for lasting modifications to occur in correlated activity ('functional plasticity') were examined in the behaving monkey. Previously, in-vitro studies of neuronal plasticity yielded important information about possible mechanisms of synaptic plasticity, but could not be used to test their functionality in the intact, behaving brain. In-vivo studies usually focused on analysis of the responsiveness of single cells, but did not examine interactions between pairs of neurons. In this study, we combined the two approaches. This was achieved by recording extracellularly and simultaneously the spike activity of several single cells in the auditory cortex of the behaving monkey. The efficacy of neuronal interactions was estimated by measuring the correlation between firing times of pairs of single neurons. Using acoustic stimuli, a version of cellular conditioning was applied when the monkey performed an auditory discrimination task and when it did not. We found that: (i) functional plasticity is a function of the change in correlation, and not of the correlation or covariance per se, and (ii) functional plasticity depends critically on behavior. During behavior, an increase in the correlation caused a short-lasting strengthening of the neuronal coupling efficacy, and a decrease caused a short-lasting weakening. These findings indicate that neuronal plasticity in the auditory cortex obeys a version of Hebb's associative rule under strong behavioral control, as predicted by Thorndike's ''Law of Effect''.

Keywords: Neuronal plasticity; Functional connection; Cross-correlation; Attention; Learning rule; Cellular conditioning

1. Introduction

Although induction of neuronal plasticity is believed to be governed by associative (James, 1890), or Hebbian-like (Hebb, 1949) rules, the exact 'learning rules' involved are not known. By 'learning rules,' we refer here to the dependence of modifications in neuronal interactions on all the parameters that may affect it, including behavioral ones. Optimally, learning rules should describe the exact conditions under which plastic changes occur in natural situations. With regard to learning rules in natural situations, basic questions that are still unanswered are: (i) what is the associative requirement: correlation (or contiguity) of firing, covariance (or contingency), or changes in either correlation or covariance; (ii) is plasticity specific to those neuronal pairs that fulfil the associative requirement; and (iii) is the associative requirement sufficient, or is there an additional necessary factor (supervisor, critic, or a general 'enabler').

Studies conducted on a variety of animal models (reviewed in Viana Di Prisco, 1984; Byrne and Berry, 1989; Brown et al., 1990; Rauschecker, 1991; Shulz et al., 1993; Fregnac and Shulz, 1994; Ahissar and Ahissar, 1994; Weinberger, 1995; Cruikshank and Weinberger, 1996b; Edeline, 1996) yielded different, and sometimes seemingly contradictory, answers to the above questions. For example, in different studies specific and non-specific, as well as supervised and non-supervised, mechanisms were demonstrated. These apparent contradictions might be, at least partially, due to the lack of control for neuronal mechanisms that are normally controlled by behavior in mammals. Most of these studies described mechanisms for plasticity that are feasible for particular neuronal tissues, and that

* Corresponding author. Tel.: +972 8 9343748; fax: +972 8 9344140; e-mail: bnehud@weizmann.weizmann.ac.il.

0028-3908/98/$19.00
PII: S0028-3908(98)00068-9

could be used during learning, but are not necessarily those actually used in the behaving mammalian brain. Since learning is a behavioral phenomenon, neuronal mechanisms underlying learning should ultimately be examined in behaving animals.

In the few studies conducted with awake animals, behavioral influences were either not investigated (Baranyi et al., 1991) or the neurons were recorded after, not during, the period in which the plastic changes were induced (Brons and Woody, 1980; Merzenich et al., 1990; Pons et al., 1991). Therefore, it was not possible to directly investigate the involvement of behavioral factors in the postulated learning rules. When neurons were recorded during behavioral conditioning (Weinberger, 1993, 1995), learning rules could not be explored since recordings were made from one cell at a time. Since most associative learning rules assume dependency on the simultaneous activities of both pre- and post-synaptic cells, simultaneous recordings of both cells are necessary. Optimally, synaptic efficacy should be measured by intracellular recording of synaptic potentials (Markram and Tsodyks, 1996). However, such recordings are extremely difficult in behaving mammals, and practically impossible in studies of neuronal plasticity that entail recordings from the same neurons over long periods of time.

In the present study, the necessary and sufficient conditions for the induction of neuronal plasticity in the behaving monkey were investigated. This was achieved by using extracellular recordings and measuring the functional efficacy of synaptic connections using cross-correlation analysis, which circumvented the technical limitations described above. The cross-correlation between the firing times of pairs of neurons is a manifestation of the net effect of the synaptic network, including direct and indirect connections that involve the two neurons. This correlation represents the so-called 'functional (or effective) connection' (Frostig et al., 1983; Aertsen et al., 1989; Ahissar et al., 1992a; Ahissar and Ahissar, 1994; Vaadia et al., 1995). Presumably, lasting changes of functional connections (functional plasticity) represent lasting changes of synaptic connections. In a previous paper concerning this study (Ahissar et al., 1992b) we showed that functional plasticity in the behaving monkey obeys a Hebbian-like associative rule, but also requires a behavioral control. Herein, the grounds of these findings are extended, and additional characteristics of functional plasticity are described. We describe here the emergence of functional connections, the specificity of functional plasticity, the time-course of the conditioning process, and the effects of the monkey's self-generated acoustic sounds on the measured functional connections. This study does not address the behavioral outcome of functional plasticity.

2. Materials and methods

2.1. Surgery and microelectrodes

Two adult male monkeys were used. Monkey A (*Macaca mulatta*, 4.5 kg) did not perform any behavioral task, and was only trained to sit quietly in a primate chair. Monkey B (*Macaca fascicularis*, 5 kg) was trained to perform an auditory discrimination task (see Section 2.5). At the end of the training period, the animals were prepared for electrophysiological recording. Surgical anesthesia was induced with an intramuscular injection of ketamin hydrochloride (Ketalar, 0.5 mg), followed by intravenous infusion of pentobarbital. The animal was then positioned in a stereotaxic device and a metallic chamber was fixed above a hole drilled in its skull to allow for a vertical approach to the primary auditory cortex (Pfingst and O'Connor, 1980). The microelectrodes, which were made in the laboratory, consisted of glass-coated tungsten with an exposed tip of 15–30 μm and impedance of 0.2–1 MΩ, measured at 1000 Hz. Five electrodes were inserted into a metal sleeve (16 gauge stainless-steel needle) so that the horizontal distances between tips were 300–600 μm. After the surgical procedure, the monkeys were allowed to recover for 3–4 days before the experimental sessions were initiated.

2.2. Recording

In each experimental session, the monkey sat in a primate chair located in an anechoic double-walled, sound-attenuating room (IAC). An array of five micromanipulators was attached to the chamber so that the five microelectrodes could be advanced together or separately into the cortex. First, the five microelectrodes were advanced together into the cortex while click stimuli (100 μs pulses, at a rate of 1 s^{-1}) were presented to the monkey. The auditory evoked potential (AEP) and the multi-unit activity were continuously examined during the insertion of the electrodes. When a negative phase in the AEP was observed, we started to advance each microelectrode separately, in steps of 100 μm. When the negative phase attenuated, and subsequently switched to positive, we advanced each electrode in 10 μm steps to isolate single-unit action potentials. Simultaneous recording of single units was achieved by utilizing spike-sorting devices that could isolate the activity from two to three single units. Five of these devices were used, two (designed and built in our laboratory) sorted spikes by shape (for details see Abeles and Goldstein (1977)), while the other three were standard dual-window discriminators (Frederick Haer and Bak).

2.3. Selection of neuronal pairs

Neuronal pairs were selected for conditioning according to the pattern of their correlated activity, as revealed by the cross-correlation histogram (CCH, Fig. 1A) that was computed from their spontaneous activities. There were four criteria for selecting pairs for conditioning: (i) there should exist a significant peak or trough near the origin of the CCH, indicative of correlated or anti-correlated activity; (ii) the width of the peak/trough should be of a few to a few tens of ms; (iii) the peak/trough should be asymmetric in relation to the origin, i.e. the area under the peak/trough on one side of the origin should be larger than that on the other side (e.g. Fig. 1A and examples of NCI, EX, and INH in Fig. 1B), presumably indicative of the involvement of unidirectional connections; and (iv) the entire peak/trough should be confined to one side of the origin (e.g. Fig. 1A and EX in Fig. 1B), presumably indicative of a unidirectional connection. Pairs that fulfilled all four criteria were selected first; those that fulfilled (i), (ii), and (iii) were selected next; those that fulfilled (i) and (ii) were selected next; and those that fulfilled only (i) were selected last. Thus, our database was biased towards asymmetrically coupled pairs.

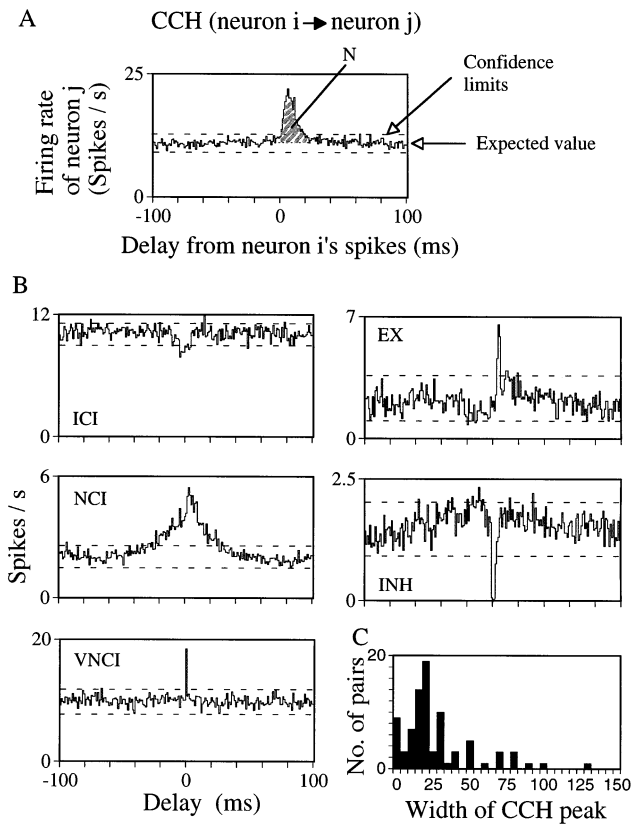

Fig. 1. (A) Calculation of the strength evaluators from the CCH. N is computed on one side of the origin and equals the number of spikes under the peak (or above the trough) and above (or below) the expected value (dotted line). For each histogram, confidence limits of 99% for the equivalent, independent Poisson processes (Abeles, 1982b) are indicated by horizontal broken lines. N, excessive spikes under the peak; $N1$, total spikes of neuron i; $N2$, total spikes of neuron j; ASG = $N/N1$; ASC = $N/N2$. (B) Examples of the different correlation types. The type of correlation (see legend of Table 1 for definitions of abbreviations) is indicated for each pair. Activities were recorded during spontaneous activity. Bin = 1 ms. Computation times: ICI, 2392 s; NCI, 600 s; VNCI 600 s; EX, 3029 s; INH, 2305 s. The NCI and VNCI pairs were recorded simultaneously. The INH pair was recorded from a single electrode, and thus, the bins (-1, 0, and 1) were bound to have close to 0 counts. (C) Distribution of the widths of the CCH peaks and troughs of 84 neuronal pairs of monkey B before conditioning.

For each group of single units (2–10 neurons, mean = 5.3), the cross-correlation matrix (CCM) was computed on-line. This matrix included all possible CCHs (off-diagonal histograms) between pairs of neurons in the group and all autocorrelation histograms (ACHs; diagonal histograms) of the neurons in the group. The CCM that was computed for spontaneous activity was examined for signs of correlated activity. When a neuronal pair that exhibited a satisfactory pattern of CCH (see criteria defined in the previous paragraph) was found, it was conditioned in one or several blocks according to the paradigms described in the following section. The firing pattern of each neuron and the pattern of the correlated activity were monitored through their respective ACHs and CCHs before, during, and after each conditioning. The on-line presentation of these histograms was useful in assessing the statistical significance of the results and the time course of efficacy changes. These parameters were used to determine the number of repetitions of each block and the time course of conditioning/extinction in each block, for as long as satisfactory isolation of single units could be maintained. Recording of each group of neurons lasted 1–4 h.

2.4. Conditioning and behavioral paradigms

The dependence of functional plasticity on the firing contingency and on behavior was tested by employing the paradigms described in Fig. 2. (Note that the psychological terms 'contiguity' and 'contingency' are analogous to the statistical terms 'correlation' and 'covariance', respectively). Contingency was controlled using a paradigm resembling that of 'cellular classical conditioning' (Kandel and Spencer, 1968; Baranyi and Feher, 1981a–c, Fregnac et al., 1988 where the activity of one neuron is regarded as the 'conditioned stimulus' (CS) and the activity of another neuron as the 'conditioned response' (CR). The connection between the two neurons (the 'CS-neuron' and the 'CR-neuron') is conditioned, namely, the contingency between their activities is modified by introducing an 'unconditioned stimulus' (US). An auditory stimulus capable of eliciting, or inhibiting, activity in the CR-neuron was employed as the US. The effect of contingency was

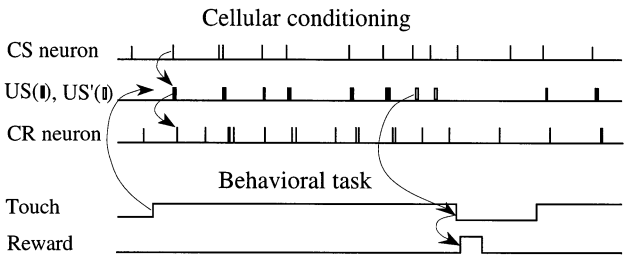

Fig. 2. The conditioning (top) and behavioral (bottom) paradigms. Each thin vertical line represents a single spike. During conditioning, the US (solid bars) was delivered immediately after the CS-neuron fired a spike. The CR-neuron usually responded to each US with one or more spikes. As a result, the contingency between the activities of the two neurons increased. Curved arrows illustrate the causal sequence. The hollow bars denote the US', an auditory stimulus different from the US, but usually still effective in activating the CR-neuron. The behavioral task is described in the text.

assessed by comparing the results of conditioning during which the contingency was changed ('conditioning') with those of conditioning during which the contingency was not changed ('pseudo-conditioning'). During conditioning, the auditory stimulus (US) was delivered immediately (2–4 ms) after the CS-neuron fired a spike, which caused the CR-neuron to fire spikes at higher (the usual case) or lower (when the CR-neuron was inhibited by the US) probability. During pseudo-conditioning, the US was delivered randomly. The conditioning period of pseudo-conditioning could only be defined de-facto when the cross-correlation between the two cells was examined and no change was found during the conditioning period. In many cases, when an acoustic stimulus could not be found that selectively activated the CR-neuron without affecting the CS-neuron, a random delivery of USs induced changes in the cross-correlations. These periods were not considered as pseudo conditioning periods. The average rate of the US, as well as all other parameters (see below), were similar in both paradigms.

The effect of behavior on functional plasticity was tested using an auditory discrimination task, during which the monkey had to attend to the US to get a reward (Fig. 2). The monkey had to touch a switch for the trial to start. Then a train of short duration (30 ms) auditory stimuli, each serving as a US in the conditioning paradigm (which was performed in parallel), was delivered. After a variable interval (0.8–2.2 s), the nature of the stimuli was changed: from a band-pass noise to a pure tone or from a lower frequency to a higher frequency tone (US (filled bars) to US' (hollow bars) in Fig. 2). If the monkey released the touch switch within 0.5 s, it received a drop of juice. The number of CS–US pairings during each conditioning block depended on the CS firing rate, the monkey's working rate, and the duration of the conditioning block. Typically, there were between 500 and 4000 CS–US pairings per block.

The combined paradigm yielded three combinations: Bhv (behavior-induced) conditioning, Non-Bhv conditioning, and Psd (pseudo)-Bhv conditioning. 'Bhv conditioning' refers to when the monkey performed the task and the functional connection between the neurons was conditioned. This paradigm yielded contingency changes that were associated with behavior. 'Non-Bhv conditioning' refers to when the trains of US were delivered in the same manner as during task performance, but the monkey was not rewarded and did not perform the task. This paradigm yielded contingency changes that were not associated with behavior. 'Psd-Bhv conditioning' refers to when the monkey performed the task, but the contingency between the activities of the two neurons was not affected. In these blocks, a pseudo-conditioning paradigm was conducted, during which the occurrence of the US was uncorrelated with the activity of the CS-neuron; the US was delivered at random times with an average rate similar to the average rate measured in the conditioning paradigm. This last paradigm yielded constant contingency that was associated with behavior.

2.5. Training

Monkey A, which did not perform any behavioral task, was trained to sit quietly in a primate chair. A drop of juice was delivered to it at random times during the training and experimental sessions.

Monkey B was trained to perform the auditory discrimination task described above. The monkey was first trained to discriminate between two fixed tone frequencies (500 and 3000 Hz). After acquisition of the fixed-tones task, the monkey was trained for generalization of the stimuli. Generalization was sequentially achieved by: training with USs of different types (see 'auditory stimuli' below), enlarging the frequency ranges of the US and US', and finally, enlarging the variability of the temporal parameters of the trials (inter-trial-interval (ITI), inter-stimulus-interval (ISI) and trial duration]. At the end of the training period, which lasted for 3 months, the monkey's degree of success at performing the task was 70–80%. Its success was deliberately kept within this range to eliminate over-training, so that the task would not be performed automatically and that the monkey would still need to improve its performance. The monkey's degree of success was controlled by manipulating the frequency difference between the discriminated stimuli and/or the ITI; decreasing the frequency differences and shortening the ITI periods lowered the success levels. Typical values for these parameters were: frequency differences of 0.5–1 octave for pure tones; overlapping frequency ranges for different types of auditory stimuli (see below); and ITI values of 0.5–1 s.

2.6. Histology

At the end of the recording sessions, the monkeys were anesthetized with pentobarbital. Stainless steel pins were inserted into the cortex of each monkey to mark the limit of the recording area. The monkeys were then sacrificed by an overdose of pentobarbital and perfused with a 10% formalin solution. A block of brain tissue that contained the whole area of the supratemporal plane was removed and cut in coronal sections of 60 μm, and the sections were Nissl stained. The core and belt areas of the auditory cortex were defined following the description of Sanides (1972).

2.7. Auditory stimuli

The auditory stimuli were delivered through a loudspeaker that was usually positioned, along the monkey's inter-aural axis, at a distance of 50 cm from the monkey's contralateral (left) ear. When the response elicited from this position of the speaker was too weak, other speaker azimuths were tried (the speaker was attached to a movable arm, see Ahissar et al., 1992b), and the one that elicited the maximal response in the CR-neuron was used.

The auditory stimulus could be one of the following types: a click (a 100 μs pulse); a white-noise (W.N., a 0–50 kHz wide-band noise); a pink-noise (P.N., a narrow-band noise with f_0 as its central frequency and a pass width of $f_0/4$); or a tone (a pure tone of f0 frequency). The intensity of the auditory stimulus was 50, 60, or 70 dB SPL (sound pressure level), when measured at 1000 Hz. The stimulus envelope, except for the click, was composed of a 10 ms increasing ramp (0–full amplitude), a 20 ms 'plateau' and a 10 ms decreasing ramp (full amplitude–0). The speaker response curve, measured at 50 and 70 dB SPL, was flat (± 1 dB) at 400–2000 Hz, attenuated at a rate of 3 dB octave^{-1} towards the lower frequencies, and flat (± 3 dB) at 2000– 30000 Hz).

In each session, the nature (type, amplitude, and frequency) of the stimulus was adjusted so as to evoke the maximal (excitatory or inhibitory) response in the CR-neuron. At the beginning of every experimental session, the frequency range of 0–30 kHz was scanned, and the best frequency(ies) was defined. The responses to all the stimulus types and amplitudes were then compared, and the best combination was chosen as the US. A stimulus that was discriminable from the US, but was still efficient in evoking a CR, was chosen as the US' (see Section 2.4).

2.8. Computer hardware and software

A microcomputer (Intel 310/386) was used to control the experimental sessions, data collection, and on-line data analysis. Both the behavioral paradigms and the cellular conditioning paradigms were controlled by the computer, which used a multi-tasking, real-time, operating system, RMX II. The conditioning paradigms were accomplished as follows. An interrupt-driven task was activated by every spike of the CS-neuron. This task immediately delivered the US (or US'), whose nature was predetermined. The overall latency from the CS spike to US onset was not longer than 4 ms. The data collection of the simultaneous recording of single units was done via a first-in-first-out (FIFO) digital sampling board that was designed and manufactured in our laboratory. This board prevented overloading of the processor by simultaneous multi-spike bursts.

2.9. Data analysis

2.9.1. Evaluation of the strength of connections

The evaluation was based on the area under the peak (or trough) of the CCH that was above or below the expected chance correlations, on one side of the origin (Fig. 1). Three types of 'strength evaluators' were used in this study: asynchronous gain (ASG), asynchronous contribution (ASC), and synchronous gain (SG) (Levick et al., 1972; Abeles, 1982a; Vaadia et al., 1991). The ASG equaled the average number of spikes added to the spike train of the CR-neuron following each spike of the CS-neuron. The ASC equaled the average number of spikes that exceeded the expected number of spikes in the spike train of the CS-neuron before each spike of the CR-neuron. The SG estimated the relative amplitude of a hypothetical postsynaptic potential generated at the CR-neuron by spikes of the CS-neuron. This calculation of the SG assumed a Gaussian distribution of postsynaptic membrane potential (for details see Abeles (1982a), Vaadia et al. (1991)). On average, the difference between the results obtained by these three evaluators was not significant. Therefore, the results will mainly be described using the ASG evaluator.

2.9.2. Quantification of the modifications in the contingency and in the strength of connections

The strengths of functional connections were distributed over wide ranges (Table 1). The wide distribution probably resulted from the variability in the number of indirect connections that contributed to the functional connections. The effect of the preconditioning values on the conditioning results was minimized by using a 'divisive,' rather than a 'subtractive,' type of evaluator. Thus, the following terms were defined:

$$\text{Contingency Factor} = \frac{\text{ASGdur}}{\text{ASGbef}}$$

$$\text{Strengthening Factor} = \frac{\text{ASGaft}}{\text{ASGbef}}$$

Table 1
Distribution of correlation types

Monkey	Electrode	Correlation types					Total pairs
		NCI 5<150	VNCI 0<5	ICI W<150	EX W<30	INH W<30	
A	Different	105 (52)	2 (1.0)	1 (0.5)	5 (2.5)		201
	Same	25 (61)			5 (12.2)	1 (2.4)	41
B	Different	112 (8)	19 (1.3)	7 (0.5)	29 (2.1)	2 (0.1)	1407
	Same	86 (28)	1 (0.4)	2 (0.7)	20 (6.5)	3 (1.1)	309
A and B	Total	328 (17)	22 (1.1)	10 (0.5)	59 (3.0)	6 (0.3)	1958

Numbers inside parentheses indicate percentages.
EX, 'excitatory' (one-sided peaks of 1–30 ms width); ICI, 'inverse common input' (double-sided troughs of <150 ms width); INH, 'inhibitory' (one-sided troughs of 1–30 ms width); NCI, 'narrow common input' (double-sided peaks of 5–150 ms width); VNCI, 'very narrow common input' (double-sided peaks or single peaks at the origin, of 1–4 ms width); W, peak widths (W were measured between points of deviation from chance correlations)

where aft stands for after conditioning, bef stands for before conditioning, and dur stands for during conditioning.

ASGbef and ASGaft were evaluated for periods of 25–100 s (depending on the extinction rate) before and after conditioning, respectively; ASGdur was evaluated for the entire conditioning period. Any qualitative artifacts generated by this normalization were ruled out by comparing the results obtained by the divisive quantifiers with the results obtained by the equivalent subtractive quantifiers (i.e. ASGdur − ASGbef; ASGaft − ASGbef). For all the results presented here, there was no qualitative difference between the results obtained by the two approaches. However, some quantitative distortions are expected with this calculation. The fact that ASGbef appears in the denominators of both SF and CF can produce an artifactual correlation between SF and CF due to random fluctuations in the ASG values (Cohen, 1995; Cruikshank and Weinberger, 1996b). For example, when ASGbef receives, by chance, an extreme value (high or low), there is a high probability that ASGdur and ASGaft will receive values that are both lower or both higher than ASGbef, respectively. However, this artifactual correlation is limited to the range of spontaneous fluctuations in ASG values. Since these fluctuations were usually an order of magnitude smaller than the plastic changes observed in this study, the effect of these artifactual correlations was negligible. Nevertheless, for each neuronal pair, the expected CF–SF correlation due to chance fluctuations of their ASG values was also tested (see Section 3 and Fig. 8C and D).

Since ASG values fluctuated with time, functional connections were defined as having a non-zero ASG if the mean ASG was consistently different from 0 during the period preceding the conditioning. In all cases where ASGbef was defined as being different from 0, both ASGdur and ASGaft had the same sign as ASGbef. Thus, in all cases the logarithms of CF and SF could be computed.

2.10. Stationarity of recording

The effect of non-stationarity, which may accompany extracellular recordings, was minimized by taking the following precautions. (1) Only neuronal pairs in which each of the neurons exhibited a stable spike shape (as determined by the spike sorters) and firing pattern (as determined by the ACH) throughout the experiment were analyzed. (2) Each neuronal pair was tested in blocks that were repeated several times, where each block contained the various conditioning paradigms. Thus, a slow non-stationary process, if it occurred, probably had a similar effect on the averaged results from different conditioning paradigms.

2.11. Self-generated acoustic sounds of monkeys—recording and analysis

Behaving monkeys produce different kinds of acoustic noises by using their lips, hands, and legs. In this study, it was of utmost importance to ascertain that what seemed to be intrinsic plastic changes in the neuronal network connectivity was not a reflection of changes in the amount of the self-generated acoustic sounds of the monkey ('SelfGen sounds'). This was tested by continuously recording the SelfGen sounds of the monkey, and then analyzing the effect of the SelfGen sounds on the neuronal plasticity. This procedure was conducted for 47 of the neuronal pairs recorded during 23 of the penetrations conducted in monkey B. The SelfGen sounds were recorded by a microphone that was positioned 20 cm above the monkey's head. The signal was amplified and filtered to the 800–10000 Hz range and delivered to a 'standard' window discriminator (Frederick Haer). The threshold levels of the window discriminator were set so as to be at the edge of the electrical noise range (the 'lower threshold') and at twice the distance from zero (the 'higher threshold'). The times of 'threshold crossing' were recorded by the real-time computer.

Table 2
Preconditioning ASG values of conditioned pairs

Monkey	Electrode	ASG values (average ± S.D.)				Total pairs
		Correlation types				
		NCI 5<150	ICI W<150	EX W<30	INH W<30	
	No. of pairs	94	2	58	4	158
A	Different	0.110 ± 0.08		0.038 ± 0.04	−0.04	
	Same	0.110 ± 0.12	−0.04	0.042 ± 0.04		
B	Different	0.050 ± 0.05	−0.045	0.030 ± 0.02	−0.023 ± 0.018	
	Same	0.063 ± 0.07		0.064 ± 0.06	−0.02	
A and B	Total	0.087 ± 0.08	−0.043 ± 0.004	0.044 ± 0.05	−0.026 ± 0.014	

For abbreviations see Table 1.

The effect of SelfGen sounds on the neuronal activity of the behaving monkey was evaluated by computing the peri-stimulus-time-histogram (PSTH) for each of the threshold levels and for each of the neurons tested. The maximal duration of the effect on the CS-neuron and on the CR-neuron was determined from these histograms. All sections of the length of the maximal duration of the effect that followed each threshold crossing were removed from the data file, and then the procedure of evaluating the changes in the strength of the connections (see above) was repeated for the 'SelfGen sound free' data files. The contribution of the SelfGen sounds to the neuronal plasticity was evaluated by comparing the results obtained from the regular data files and the 'SelfGen sound free' data files. The use of two thresholds for the SelfGen sound recordings provided a basis for extrapolation of the results of this analysis to the range of acoustic sounds with amplitudes smaller than the electrical noise level, and hence, which could not be recorded. Such an extrapolation would be necessary if the contribution of the SelfGen sounds recorded with the lower threshold was significant (see Section 3).

3. Results

3.1. Functional connectivity

In this study, 71 successful penetrations were conducted in the right temporal lobes of two adult monkeys (12 in monkey A and 59 in monkey B). The recordings were performed from all cortical layers. In monkey A, the recordings were horizontally confined to an area of 2.5 mm (medio-lateral) × 1 mm (rostro-caudal) in the posterior region of the primary auditory cortex (AI), and in monkey B, to an area of 5 mm × 5 mm that contained both the posterior part of AI and the postauditory (PA) cortex (Jones and Burton, 1976).

The 145 neuronal groups that were recorded contained 792 neurons ('single units'). Each simultaneously recorded neuronal group contained 2–10 neurons (5.3 on average). CCHs were computed for each neuronal pair in the group. Of the 1958 neuronal pairs studied, 235 pairs were studied for conditioning effects: 79 pairs in monkey A and 156 pairs in monkey B.

CCHs were usually computed for delays from −100 to +100 ms. The strengths of functional connections were always computed in one direction (e.g. from neuron i to neuron j), according to the area under the peak, and above or below chance correlation, on one side of the origin (Fig. 1A). 'Classical' grouping by shape (Perkel et al., 1967; Moore et al., 1970; Aertsen et al., 1989; Vaadia et al., 1991) of the functional connections yielded the distribution described in Table 1 (see Fig. 1B for illustrative examples). Of the 235 pairs subjected to the conditioning paradigms, 158 exhibited functional connections prior to conditioning. The widths of the CCH peaks of these pairs were typically ≤50 ms (Fig. 1C). The average ASG values exhibited by these neuronal pairs before conditioning (Table 2) demonstrate the low contingency typically observed between the firing times of pairs of cortical neurons. The CCHs of the other 77 pairs were flat before conditioning.

3.2. Functional plasticity caused by conditioning associated with behavior

The results of a Bhv conditioning paradigm are illustrated in Fig. 3. A neuronal pair that did not exhibit correlated activity before conditioning (Fig. 3, upper left CCH; here, and in the following figures, the numbers on the right relate to $t=0$, which is the moment when conditioning ended) became strongly coupled after 100 s of Bhv conditioning (middle left CCH). This strong connection was extinguished after 50–75 s of spontaneous activity. The process (that is,

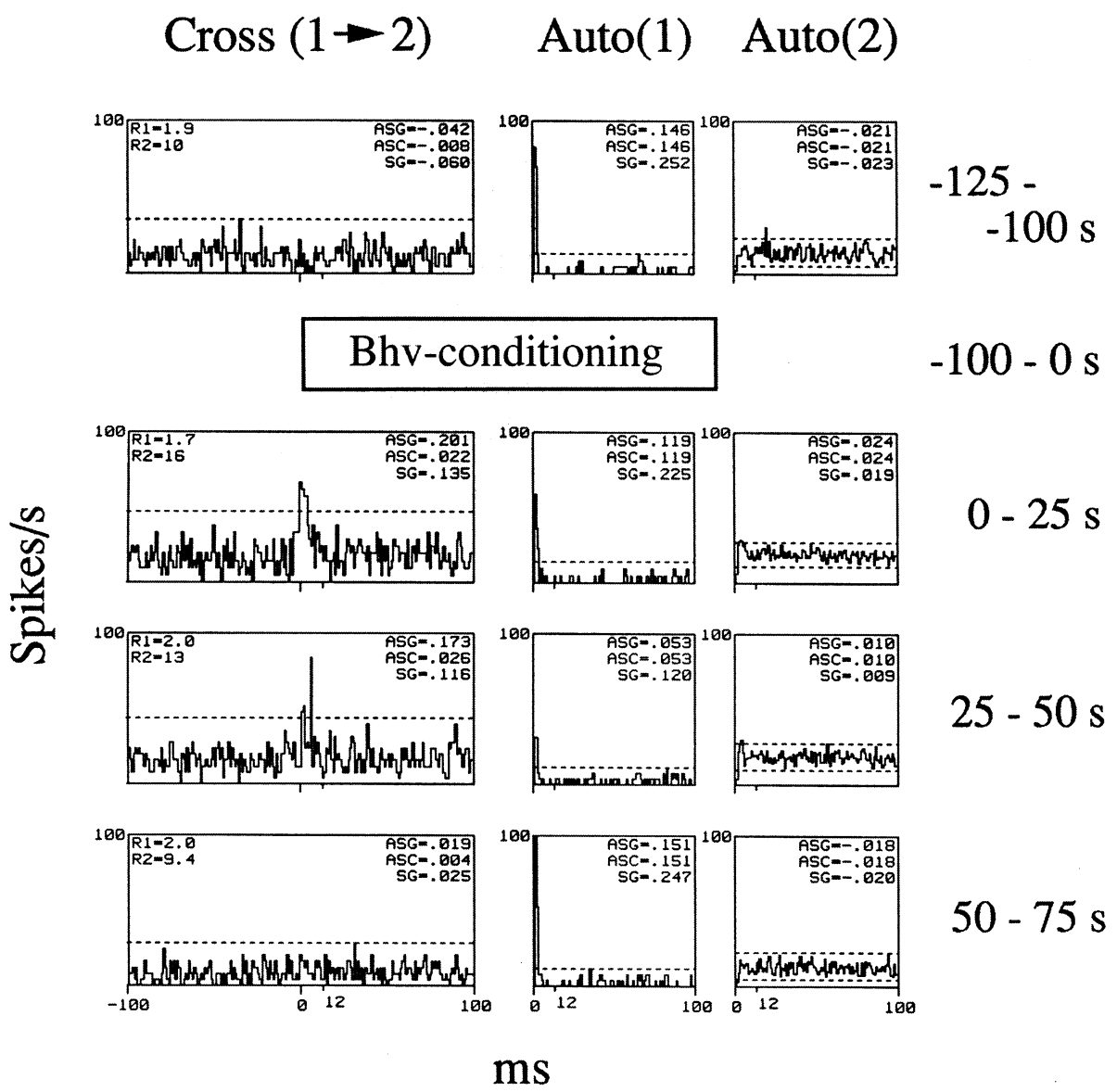

Fig. 3. An example of functional plasticity. The CCHs and ACHs of 2 neurons that were recorded from two different electrodes, while the neuronal pair was being conditioned by 5 blocks of Bhv-conditioning. US: W.N., 60 dB; US': 3 kHz, 60 dB. Histograms represent the averages of all 5 blocks. Thus, each histogram was computed from 125 s (25 s × 5) of spontaneous activity. Upper row: 25 s before conditioning. Second row: 25 s immediately after Bhv conditioning. Third row: the next 25 s. Fourth row: the following 25 s. Times to the right refer to end of conditioning, which occurred at $t = 0$. $R1$ and $R2$, average firing rates of the triggering and of the other cells, respectively, during the period computed. ASG, ASC and SG are strength evaluators (see Section 2). In this and the following figures, evaluators (ASG, ASC, and SG) were computed for delays between 0 and a certain delay (12 ms in this figure), indicated by the small vertical line to the right of the origin. Strength evaluators that were computed for the ACHs were used to quantify aspects of firing patterns. The bin widths of the CCHs and ACHs here, and in the subsequent figures, are 1 ms.

conditioning, strengthening and extinction) was repeated five times, and the figure represents the average CCHs computed over the five blocks. The minor changes observed in the ACHs (2 right columns) cannot explain the qualitative changes observed in the CCHs.

The correlation patterns that occurred during the conditioning period are depicted in Fig. 4. During a pseudo-conditioning period that was performed prior to the conditioning period (upper row), the correlation between the cells was hardly affected (right CCH), even though the CR-neuron responded to the US (middle CCH). This is because during this period, the US was not paired with the activity of the CS-neuron (left CCH), and the CS-neuron did not respond to the US. During the first 40 s of the conditioning period (middle row), the US was paired with the activity of the CS-neuron (left CCH), and as a result, the response of the CR-neuron (middle CCH) was also paired with the activity of the CS-neuron (right CCH). The resulting increased contingency is represented by the large peak

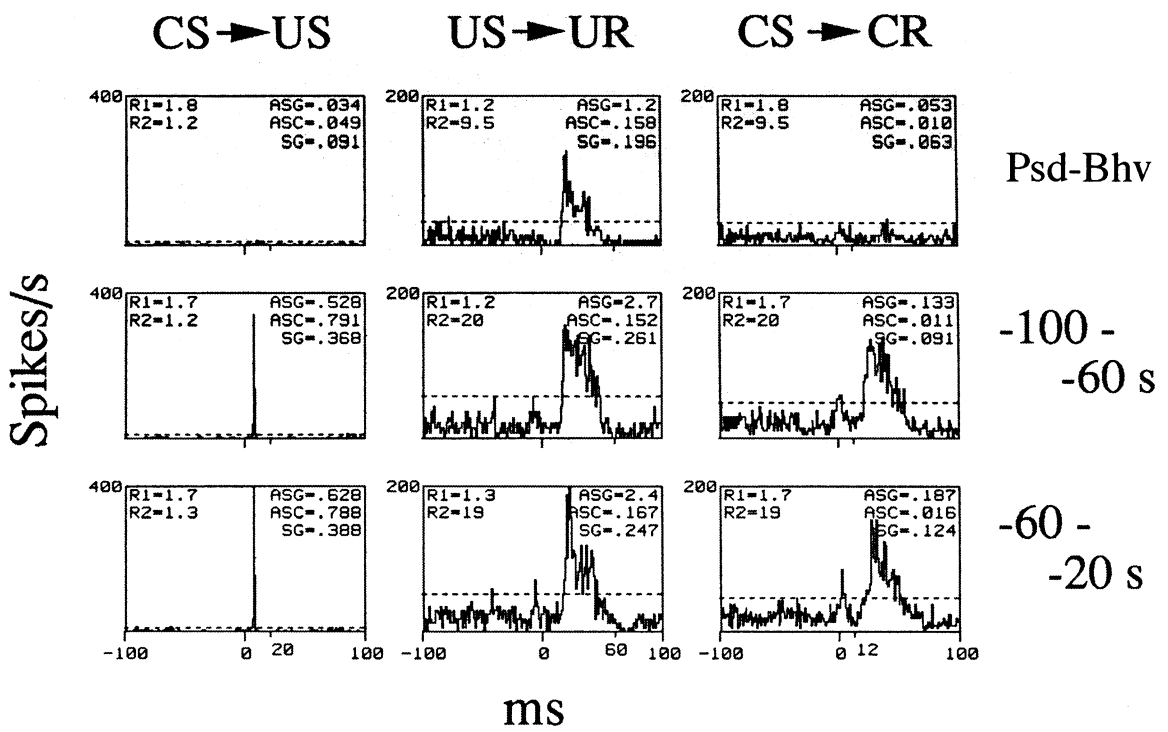

Fig. 4. Evolution of a functional connection during the Bhv conditioning period. The CCHs were computed for the same neuronal pair as in Fig. 3. US: W.N., 60 dB; US': 3 kHz, 60 dB. Left column: CCHs between the CS-neuron and the US onset. Middle column: CCHs between stimulus onset (US) and spikes of the CR-neuron (UR); these CCHs represent post-stimulus-time-histograms (PSTHs). Right column: CCHs between the two neurons (CS- and CR-neurons). Upper row: CCHs during a Psd conditioning block (computation time 120 s). Middle row: CCHs during the first 40 s of the Bhv conditioning, averaged over 3 blocks (total time 120 s). Lower row: CCHs during the next 40 s of the Bhv conditioning, averaged over 3 blocks (total time 120 s). The end of the conditioning occurred at $t = 0$. Evaluators were computed for delays between 0 and 20 ms (left), 60 ms (middle), and 12 ms (right columns).

in the CCH that starts about 20 ms to the right of the origin. This 20 ms delay is the sum of: (i) the latency between the spike of the CS-neuron and the onset of the US, and (ii) the response latency of the CR-neuron. During these first 40 s of conditioning, a small peak emerged near the origin (second row, right CCH), which represented the emergence of a functional connection between the neurons. During the second 40 s of the conditioning period (bottom row), this functional connection was further strengthened (right CCH).

Plastic modifications by Bhv conditioning occurred with all classes and strengths of functional connections. Some examples are depicted in Fig. 5. Pair 1 (Fig. 5, left CCHs) exhibited a relatively strong coupling already before conditioning, but was further potentiated by Bhv conditioning. Pair 2 in Fig. 5 (second column of CCHs) exhibited a slight anti-correlated activity before conditioning. During Bhv conditioning, this 'inhibitory' connection was strengthened, and a 'trace' of this strengthening out-lasted the conditioning period (Fig. 5, pair 2, third row), and was extinguished later. Functional connections could also be depressed. For example, a neuronal pair that originally exhibited a relatively strong and highly synchronized connection (Fig. 5, pair 3, third column of CCHs) was depressed during Bhv conditioning. As a result, the connection remained depressed after the conditioning ceased (third row), and this depression was extinguished during the following 100–150 s of spontaneous activity. Occasionally, a change in the functional connection of a neuronal pair was not accompanied by changes in the average firing rate of either of the neurons (Fig. 5, pair 4, right CCHs). Although this was not typical, it implies that at the cellular level functional plasticity and changes in cellular excitability are independent processes. Statistical support for this latter implication will be described below (see Section 3.7).

3.3. Dependence of functional plasticity on the behavior and on the contingency.

In this study, our main goal was to determine the conditions that are necessary for functional plasticity. The following example illustrates our main finding. The results of three conditioning paradigms (conditioning associated with behavior (Bhv; left CCHs), non-behavioral conditioning (Non-Bhv; middle CCHs) and pseudo- conditioning (Psd-Bhv; right CCHs); see Section 2 and Fig. 2) performed on the same neuronal pair are illustrated in Fig. 6. A relatively weak connection

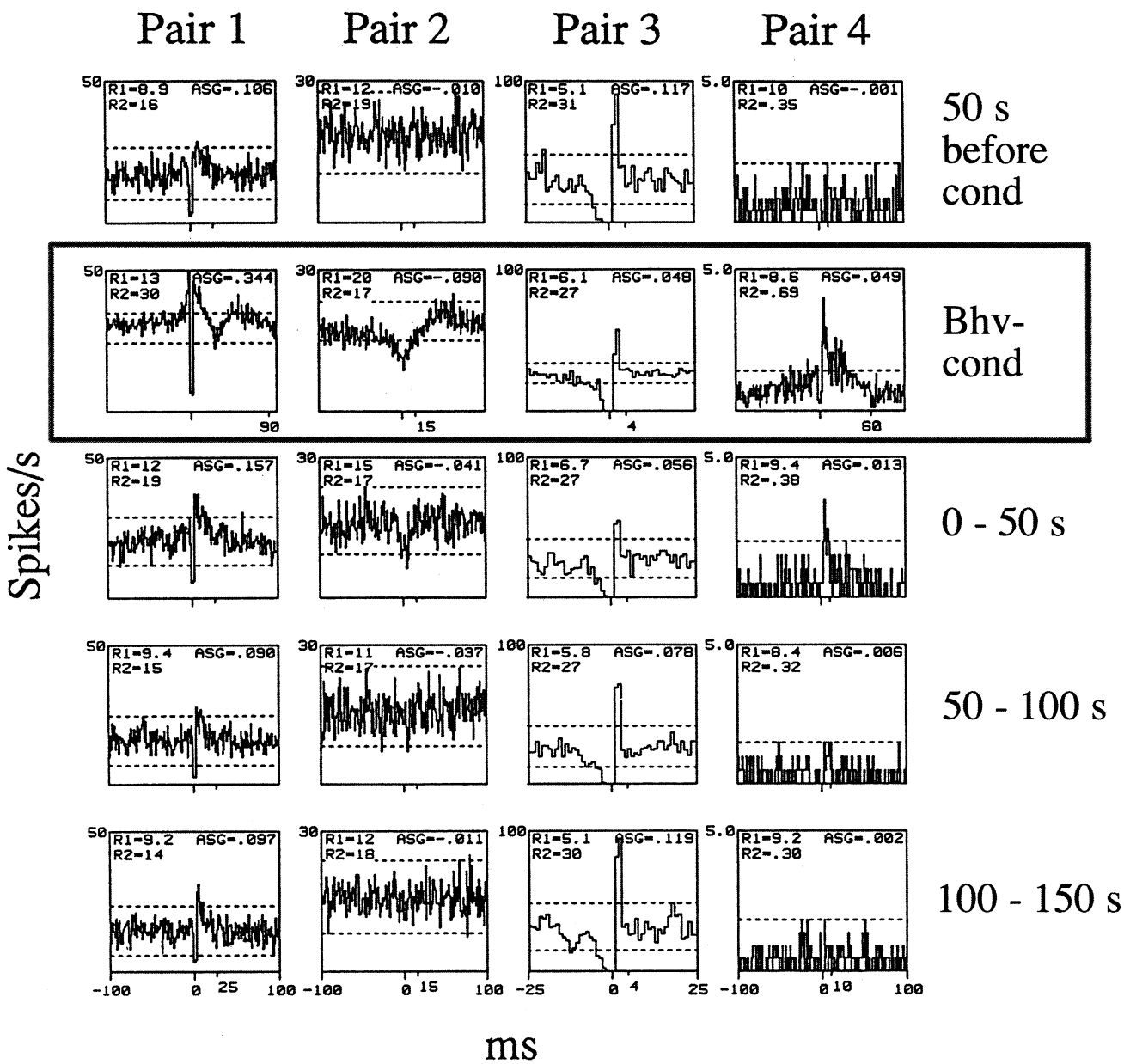

Fig. 5. More examples of Bhv conditioning. The CCHs were computed for four different neuronal pairs recorded in different penetrations. Pair 1: recorded from the same electrode; conditioning, 70 s × 3 blocks; US: 450 Hz, 60 dB; US': 550 Hz, 60 dB. Pair 2: recorded from different electrodes; conditioning, 140 s × 3 blocks; US: W.N., 60 dB; US': 3 kHz, 60 dB. Pair 3: recorded from the same electrode; conditioning, 150 s × 3 blocks; US: W.N., 70 dB; US': 300 Hz, 70 dB. Pair 4: recorded from the same electrode; conditioning, 220 s × 5 blocks; US: 200 Hz, 60 dB; US': 2 kHz, 60 dB. The 1–2 ms troughs at the origins of the CCHs of pairs 1, 3, and 4 are due to the inability of our system to detect spikes that are generated simultaneously by two neurons recorded by the same electrode. In this and all subsequent figures, stimuli were applied only during conditioning periods (second row).

(upper row) was conditioned (second row) using the three paradigms. Contingency alone (Non-Bhv) or behavior alone (Psd-Bhv) did not cause any significant change in the strength of the connection. Only the combined paradigm (Bhv) yielded a significant potentiation (~ 3 fold) of the connection's strength. This potentiation was extinguished during the following 100–200 s of spontaneous activity. The figure presents average CCHs from 2 conditioning blocks.

When a US that did not activate the CS-neuron could not be found for a particular neuronal pair, pseudo conditioning could not be achieved. Instead, an intermediate level of correlation was induced during the 'Psd-Bhv' paradigm; a correlation that represented the simultaneous responses, and thus, was expressed near the CCH's origin (Fig. 7, second row). In these cases, the plastic modifications were also of intermediate levels (third row), and were usually proportional to the correlation that was induced during conditioning.

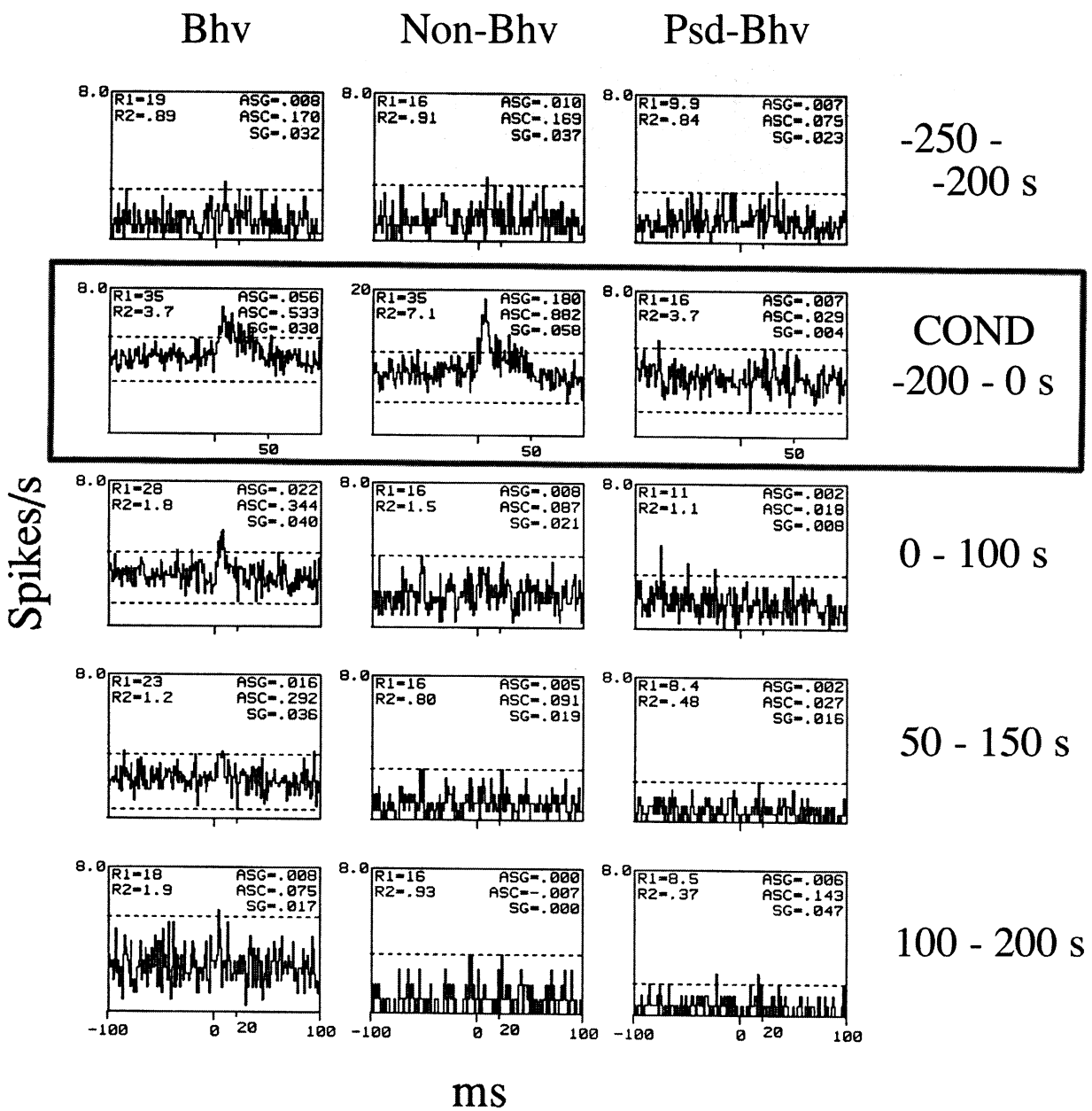

Fig. 6. Necessity of behavior and contingency for functional plasticity. A neuronal pair that was recorded by two different electrodes was conditioned twice by each of the three paradigms. US: W.N. + click, 60 dB; US': 3 kHz, 60 dB. CCHs represent the averages over the 2 blocks. Note the partial overlap of computation times during extinction, and the different scale used for the computation of the CCHs during the Non-Bhv conditioning. Other details as in the legend for Fig. 3.

Conditioning strengths differed largely between different neuronal pairs, which resulted in a wide distribution of CF values (0.1–60). The dependence of the SF on the CF in behaving and in non-behaving conditions was examined (Fig. 8). When conditioning paradigms were carried out during behavior (Fig. 8A), a clear dependency of strengthening on contingency was seen. However, when behavior was not involved (Fig. 8B) similar changes of the contingency yielded smaller, although statistically significant (see the legend of Fig. 8 and Table 3), changes in the strength of the connections. Fig. 8 thus summarizes the clear dependency of the functional plasticity on both contingency and behavior.

The linear curve-fitting (on a log–log scale) for the data in Fig. 8 suggests a single power-law modification rule, namely $SF \approx CF^{1/2}$, which describes both potentiation and depression, in agreement with previous results (Fregnac and Shulz, 1989). Such a rule can account for 66% of the data variance. Alternatively, SF could be a non-smooth function of CF, due to some threshold mechanisms (Artola et al., 1990). For demonstration of

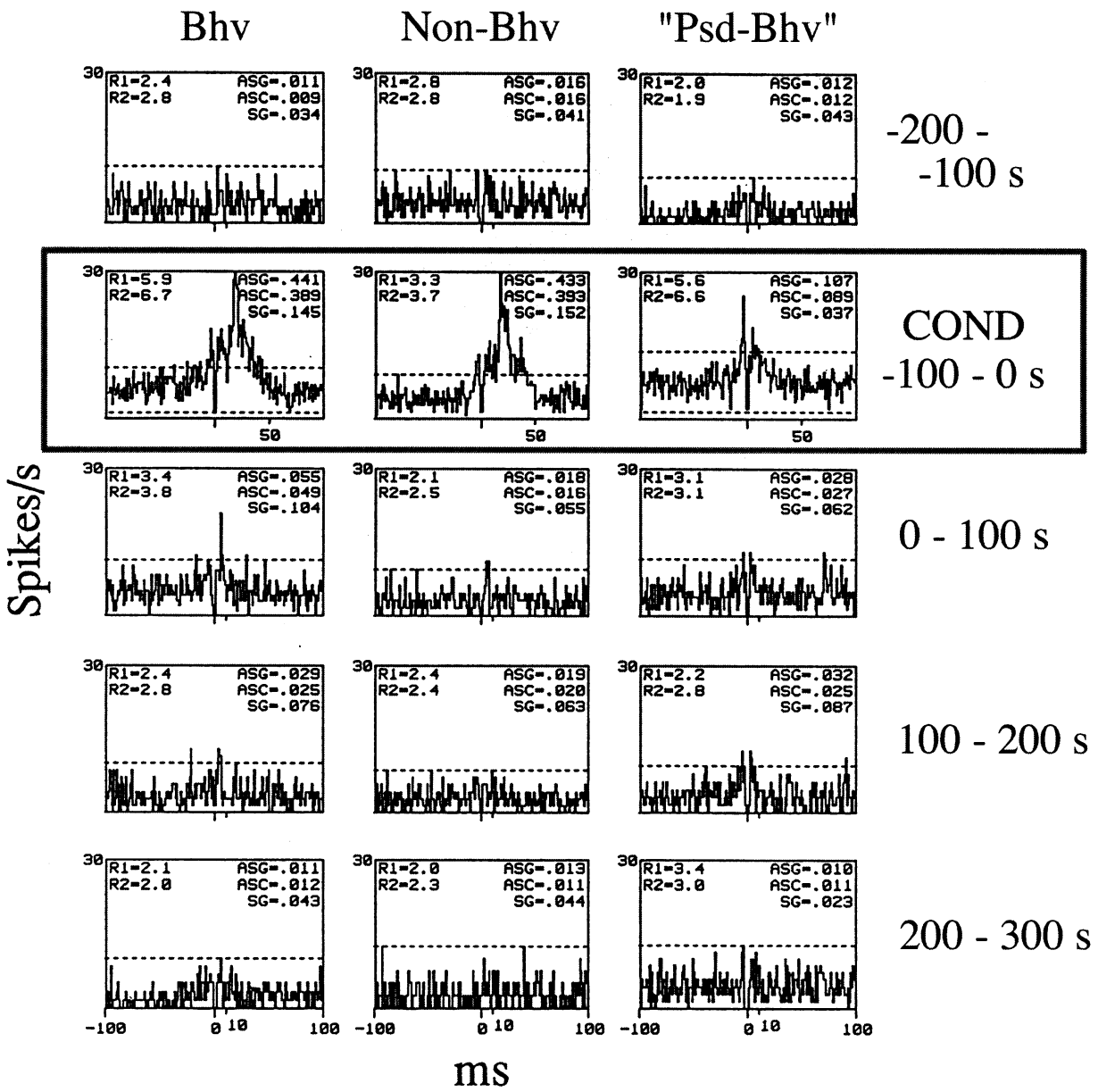

Fig. 7. Dependence of strengthening on contingency level. A neuronal pair that was recorded by a single electrode was conditioned three times by each of the three paradigms. US: 150 Hz, 70 dB; US': 300 Hz, 70 dB. The CCHs represent the averages obtained over the 3 blocks. Psd-Bhv conditioning induced an increased correlation due to simultaneous responses of both neurons to the US, which was not paired with either neuron.

such a possibility, the CF continuum was divided into three regimes: potentiating (Pot), pseudo (Psd), and depressing (Dep). On a heuristic basis, we defined Pot as $CF = 2$, Dep as $CF \leq 0.5$, and Psd as $0.5 < 2$. Three independent curves were fitted for the three conditioning regimes (Fig. 8, thick lines); power-law curves fitted the Pot and Dep regions, while a polynom of the fifth order fitted the Psd region. The degree of the polynom was chosen as the degree above which the R.M.S. error was saturated. For the behavioral condition, the regional curve fitting describes a sigmoid-like function, with a threshold for potentiation between $CF = 1.5$ and $CF = 2$. Determination of the threshold for depression, and of the exact characteristics of the region around $CF = 1$, requires additional data.

The average values for the parameters of the different conditioning categories are presented in Table 3. Although the average values for CF were similar in both behaving and non-behaving conditions, the average values of the SF were significantly different between these two behavioral conditions following both the Pot and Dep conditioning. Pot-Bhv and Dep-Bhv yielded 2.8- and 2-fold modifications, respectively, of the original ASG values, while Pot-Non-Bhv and Dep-Non-Bhv yielded only about 1.3-fold modifications. The differences between the results of the two behavioral condi-

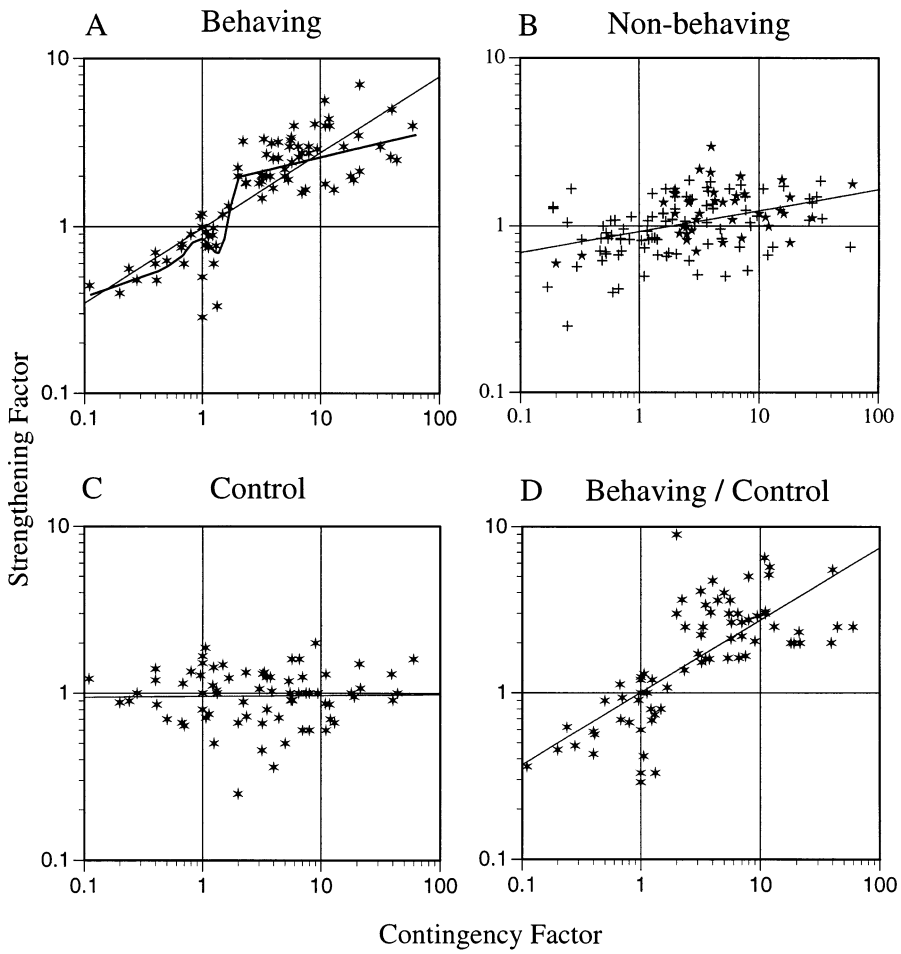

Fig. 8. Dependence of the strengthening factor on the contingency factor and on the behavioral condition. Data was gathered from both monkeys A and B. Each star represents the average value for one conditioning paradigm of one neuronal pair. Seventy-nine pairs from monkey B were conditioned; 65 during behavior (20 of them with two different CF values); 39 during non-behaving periods; and 25 were conditioned in both behavioral conditions. Seventy-nine pairs from monkey A were conditioned during non-behaving periods only, 11 of them with two different CF values. (A) Bhv conditioning (monkey B). Curve fitting (thin line): $SF = 0.98\ CF^{0.45}$, $r = 0.81$, $P < 0.0001$, $n = 85$ (65 pairs). Regional curve fitting (thick line): $SF = 1.9CF^{0.17}$, $CF \geq 2$; $SF = 9.4 - 50CF + 107CF^2 - 105CF^3 + 48CF^4 - 8.2CF^5$, $0.5 < 2$; $SF = 0.72CF^{0.25}$, $CF \leq 0.5$. (B) Non-Bhv conditioning. monkey A (+) and monkey B (*). Curve fitting (thin line): $SF = 0.93\ CF^{0.13}$, $r = 0.41$, $P < 0.01$, $n = 129$ (118 pairs). (C) Expected CF–SF correlation due to spontaneous fluctuations of ASG values (see Sections 2 and 3). Each star represents data as in panel A, except that instead of ASGaft, an ASG value, which was computed from a period just before the subsequent conditioning block, was used. (D) Replotting of the data in panel A after dividing the value of each data point by its corresponding value in panel C.

tions were statistically significant ($P < 0.0001$) in both the Pot and Dep cases. There was no significant difference between the effects of the pseudo-conditioning applied during the behaving and the non-behaving conditions. Finally, in both the behaving and the non-behaving conditions, each of the three conditioning regimes yielded results that were significantly different from those obtained with conditioning in the other two regimes ($P < 0.0001$), except for Psd-Non-Bhv and Dep-Non-Bhv. However, this latter lack of significance could be due to the small sample that was available.

Since ASGbef appears in the denominators of both CF and SF, an artifactual correlation between CF and SF could be generated due to spontaneous fluctuations of ASG values (see Section 2, Cohen, 1995; Cruikshank and Weinberger, 1996b). Therefore, the expected CF–SF correlation due to chance fluctuations of their ASG values was tested. For each neuronal pair and each Bhv conditioning block, the SF was computed again, but with replacing ASGaft by the ASG value measured just before the next conditioning block. Since the onset times of the consequent conditioning were determined arbitrarily, but always after the extinction process of the previous conditioning had terminated, these values represent randomly-selected spontaneous ASG values. The CF–SF correlation that emerged from these spontaneous fluctuations was negligible (Fig. 8C). However, the range of the SF values in Fig. 8C indicates that the depression values observed in Fig. 8A might emerge from spontaneous fluctuations. This point was further tested by dividing the value of each data point in panel A by its corresponding control value in panel C (Fig.

Table 3
Average results of conditionings in the different CF regimes

Conditioning	Behaving			Non-behaving		
	Dep	Psd	Pot	Dep	Psd	Pot
Contingency	CF ≤ 0.5	0.5 < 2	CF ≥ 2	CF ≤ 0.5	0.5 < 2	CF ≥ 2
No. of pairs	7	25	53	14	37	78
CF (average ± S.D.)	0.3 ± 0.1	1.1 ± 0.3	11 ± 12	0.3 ± 0.1	1.1 ± 0.3	10 ± 11
SF (average ± S.D.)	0.5 ± 0.1*	0.9 ± 0.3	2.8 ± 1.1**	0.8 ± 0.4**	0.9 ± 0.3	1.3 ± 0.5**
ASG change*** (average ± S.D.) (%)	−50 ± 10	−10 ± 30	+180 ± 110	−20 ± 40	−10 ± 30	+30 ± 50

Dep, depressing conditioning; Psd, pseudo-conditioning; Pot, potentiating conditioning.
* $P < 0.005$; ** $P < 0.0001$, one tailed t-test; *** ASG change, average percentage of change in ASG compared with the initial ASG value, following conditioning.

8D). The differences between Fig. 8A and Fig. 8D are negligible.

3.4. Differential conditioning

The clear dependency of strengthening on the induced increment in correlation indicates that the functional plasticity associated with behavior was specific; only neuronal pairs for which contingency was increased were potentiated, and only those for which contingency was decreased were depressed (Fig. 8A). This specificity is demonstrated for three neurons that were simultaneously conditioned (Fig. 9). Neurons 9 and 10, which were recorded from the same electrode, showed a relatively strong spontaneous functional coupling. Neuron 4, which was recorded from a different electrode, was weakly correlated with neuron 10, and not at all with neuron 9. During Bhv conditioning, only the connection from 4 to 10 was potentiated. As a result, only this connection showed lasting potentiation.

3.5. 'New' functional connections following conditioning

Cross-correlation is not sensitive enough to detect very weak connections, since this correlation is computed over a limited period of time. Thus, a 'flat' CCH may 'hide' a weak connection buried in the noise. Sufficient strengthening of such 'hidden connections,' can make them 'visible' to the cross-correlation technique.

Pot-Bhv conditioning were applied to 77 neuronal pairs (those not included in Table 2) that exhibited a 'flat' CCH. Of these pairs, 18 (23%) exhibited functional coupling after conditioning: 14 (18%) exhibited an 'excitatory' (e.g. Fig. 3 and pair 4 in Fig. 5) and 4 (5%) an 'inhibitory' (e.g. pair 2 in Fig. 5) connection. All modifications were extinguished during several minutes of spontaneous activity. Pot-Non-Bhv conditioning potentiated only 4% (3/73) of the tested 'flat' pairs. Conditioning in other CF regimes did not cause any detectable change in the 'flat' connections.

3.6. Time course of conditioning processes associated with behavior

The duration of the conditioning periods varied from 70 to 900 s. The observed extinction durations, measured between the end of the conditioning and the moment at which the ASG returned to preconditioning value, varied between 50 and 650 s. These two parameters were strongly correlated ($r = 0.7$, $P < 0.0001$), with extinction typically lasting for about 2/3 of the conditioning duration. In contrast, extinction duration was not significantly correlated with any of the following parameters: CF, SF, ASGbef, ASGaft, average firing rates, changes in average firing rates during conditioning, or recording distance (i.e. neurons recorded from the same versus different electrodes).

Except for their time scales, the dynamics of modifications were similar for different conditionings. A typical example for the dynamics of the short-term plastic modifications observed in this study is presented in Fig. 10. The conditioning (and extinction) durations in this example were atypically long for this study. This neuronal pair exhibited a spontaneous functional coupling of a typical ASG value (Fig. 10A, upper CCHs; Fig. 10B, upper trace). This connection was potentiated four times by Bhv conditioning (for 10–15 min) and once by Non-Bhv conditioning (for 10 min; Fig. 10B). Following each of the conditioning periods, the connection remained potentiated, and this potentiation was extinguished during several minutes of 'spontaneous' activity. In this example, the correlation that was induced during the Non-Bhv conditioning was smaller than that induced during the Bhv conditioning (Fig. 10B, upper trace). Although this difference was not typical for this study (see Fig. 8 and Table 3), the difference between the amount of plasticity induced by these two paradigms (Fig. 10A) was.

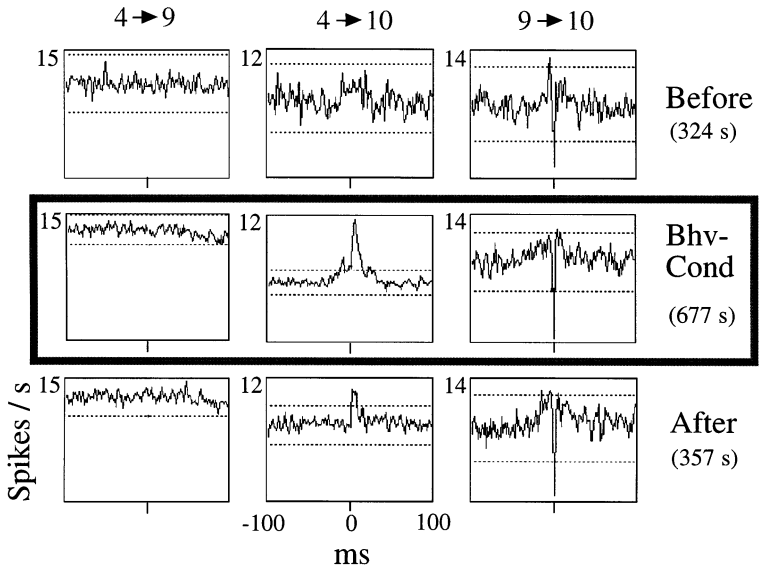

Fig. 9. Differential conditioning. Three neuronal pairs were simultaneously conditioned. US: W.N., 70 dB; US': 3 kHz, 70 dB. During Bhv conditioning, the correlation between neurons 4 and 10 was increased while the correlations between the other two pairs were hardly affected. As a result, only the connection between neuron 4 and 10 showed lasting potentiation.

3.7. Cellular excitability changes

The general excitability of an extracellularly recorded neuron is usually estimated by measuring the average firing rate of the neuron. When averaged over the neurons studied, the 'spontaneous' average firing rate was elevated by 20.2% following Bhv conditioning and by only 0.7% following Non-Bhv conditioning.

Changes in excitability could potentially explain changes in inter-neuronal correlations without synaptic modifications. Such a mechanism should: (i) lead to plastic modifications that are not specific to the CS-neuron, and (ii) be accompanied by a significant correlation between changes in the average firing rates and changes in the coupling strengths. The first prediction was not supported by our data (see Figs. 8 and 9 and Section 3.4). The second prediction was tested by examining the pairwise correlations between the SF and the changes, induced by the conditioning, of the firing rates of the two neurons ($R1$aft/$R1$bef and $R2$aft/$R2$bef; where $R1$ and $R2$ are the firing rates of the CS- and CR-neuron, respectively). No significant correlation was found between the SF and the induced changes in the firing rates of either the CS-neuron ($r = 0.14$, $P > 0.1$) or the CR-neuron ($r = 0.19$, $P > 0.05$). Thus, although the population trends were correlated (connections were strengthened and firing rates were elevated), single pair modifications (strengths and rates) were not, which indicates that changes in neuronal couplings were not due to changes in general cellular excitability.

3.8. Effect of self-generated acoustic sounds of the monkey

The acoustic stimuli that were initiated by the experimental machinery were not the only acoustic stimuli that the monkey heard. During task performance and in between trials, the SelfGen sounds (see Section 2) often effectively activated the cortical neurons that were studied. These SelfGen sounds were produced at an elevated rate during behavioral conditioning, and their rate gradually declined during 25–100 s after the conditioning ceased. Thus, the CCH of two neurons that respond to the SelfGen sounds may exhibit an apparent functional connection, which is actually a reflection of the responses of the neurons. Such a pair might exhibit a 'plasticity' that is a reflection of the rate changes of the SelfGen sounds and not of synaptic modifications. Thus, what seems like plastic changes in the connectivity of the neuronal network may be nothing more than changes in the amount or nature of the SelfGen sounds being reflected in the neuronal activity. This possibility was examined by applying the tests described in Section 2 to 47 neuronal pairs in 63 blocks of the Pot-Bhv, Pot-Non-Bhv, and Psd-Bhv conditioning paradigms. Briefly, we produced 'SelfGen-sounds free' ('silence only') data files for all these blocks, analyzed these files, and compared them with the results obtained with the intact data files ('regular'). The differences between the average values of strengthening obtained using the intact data files and the 'silence only' (low threshold) data files were not statistically significant ($P > 0.2$). Thus, SelfGen sounds did not significantly influence functional plasticity. A pair-wise comparison (Fig. 11) of all

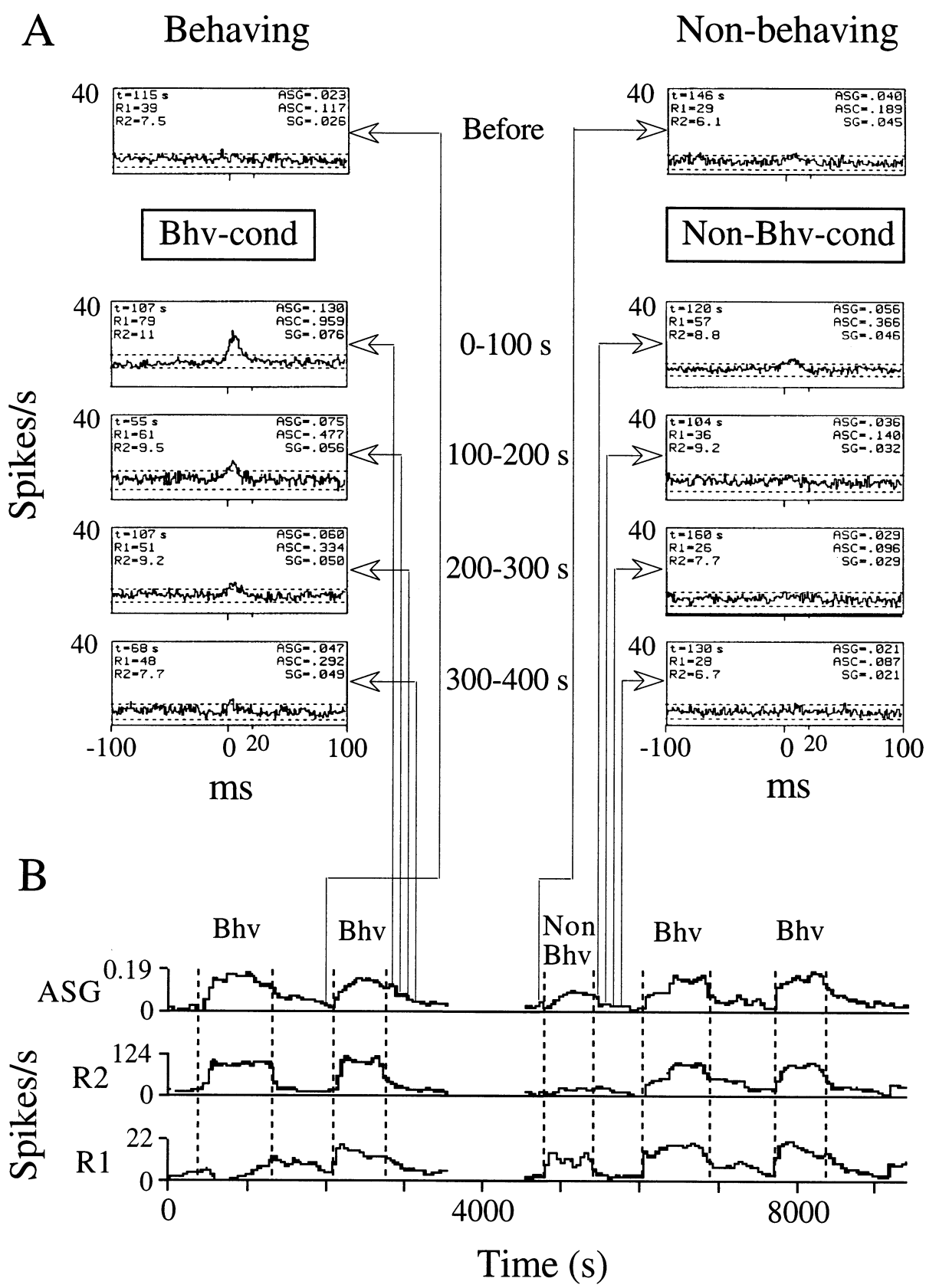

Fig. 10. Time-course of functional plasticity. A neuronal pair that was recorded from two different electrodes was conditioned during five consecutive blocks (four Bhv and one Non-Bhv). (A) CCHs computed from different time points before and after two conditioning blocks: a Bhv conditioning (left CCHs) and a Non-Bhv conditioning (right CCHs). The time points are indicated in B. Computation times are indicated within each CCH as 't'. (B) Time-course of the ASG and the average firing rates of the triggering and the other neuron ($R1$ and $R2$, respectively). Values were averaged over periods of 100 s every 50 s (with a 50 s overlap). The neuronal pair was recorded continuously for the 9481 s depicted, with a break of about 15 min around $t = 4000$. Spike shapes and sorting quality were constant during the entire recording period. Conditioning occurred between each pair of vertical dashed lines, as indicated.

single cases showed that in only a few cases were the effect of the SelfGen sounds prominent. A linear regression line with a slope of 0.88 explains most of the effect ($r^2 = 0.55$).

A typical case is illustrated in Fig. 12 (same neuronal pair used for Figs. 3 and 4). With this neuronal pair, the effects of the SelfGen sounds lasted less than 20 ms. Thus, 20 ms intervals following each occurrence of the SelfGen sounds were removed from the data files. This process was repeated for both sound thresholds. In this example, the main effect of removing the intervals of SelfGen sounds was to reduce the width of the correlation peak (Fig. 12, second row). A slight weakening of the strength of the connections was also evident. However, the partial elimination of the intervals of SelfGen sounds (middle column) yielded more weakening than elimination of all the recorded SelfGen sounds (right column). Qualitatively the process of functional plasticity looks similar, whether or not the intervals of SelfGen sounds sections are included.

4. Discussion

Cross-correlations between firing times of extracellularly recorded spikes of single neurons were utilized to study the rules that govern plasticity in local cortical circuits. This approach enables the study of the role of behavioral factors in cortical plasticity. However, it precludes the direct measurement of synaptic potentials, and thus the direct measurement of synaptic plasticity. Obviously, this approach can not replace intracellular measurements. However, it bridges the gap that exists between studies at the intracellular level and at the behavioral level. The approach we present here provides critical tests of predictions from behavioral studies, and constrains interpretations of intracellular studies.

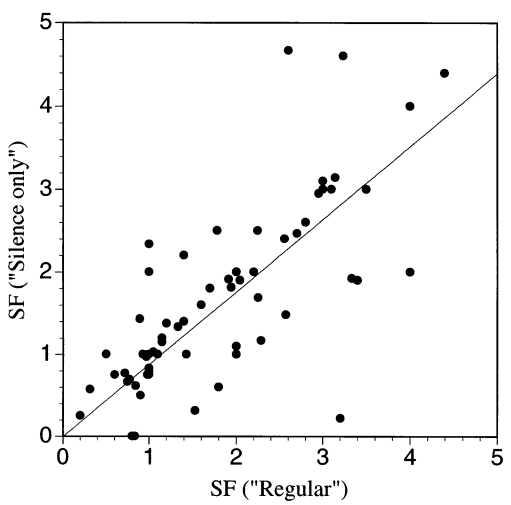

Fig. 11. Effect of the removal of the monkey's SelfGen sounds. Each star represents the average value for one conditioning paradigm of one neuronal pair (Monkey B, 63 conditionings, 47 pairs). The x-axis represents SFs computed from the intact ('regular') data files. The y-axis represents SFs computed from the data files from which SelfGen sections were removed ('silence only').

4.1. Interpretations of neuronal cross-correlations

The CCH between a pair of cells in a given neuronal network can be unequivocally calculated for each period of activity. However, this does not hold for the reversed mapping. Different synaptic networks can produce similar CCHs. For example, if the CCH shows that cell A tends to fire before cell B, there are alternative interpretations. One interpretation is that there is an excitatory synapse from A to B, and another is that cell A belongs to a neuronal group that tends to fire before a neuronal group that contains cell B, but that there is no direct synapse between the two cells. Rules of thumb to discriminate between direct and indirect connections according to the shape of the CCH had been suggested over the years (Moore et al., 1970; Dickson and Gerstein, 1974; Fetz and Gustafson, 1983). However, simulations of neural networks showed that false detection rates by such rules of thumb are not small (Bedenbaugh et al., 1988; Gerstein et al., 1989; Boven and Aertsen, 1990). For example, when neuronal circuits with known connections were simulated, in about half of the cases in which the CCH peak was confined to one side of the origin there was no direct connection between the neurons (E. Ahissar, unpublished observations). Therefore, actual synaptic connectivity probably cannot be deduced from CCHs. However, functional connectivity, that is, the expression of the synaptic connectivity at the inter-neuronal correlated activity, can be determined directly from CCHs. CCHs reflect the statistical efficacy of the coupling between two neurons, mediated by both direct and indirect synaptic connections (Aertsen et al., 1994). The information contained in CCHs relates directly to activity covariance, mutual information, and surprise functions, all of which were suggested by both theoretical accounts (Uttley, 1976; Sejnowski, 1977; Aertsen et al., 1989; Levy, 1989; Eggermont, 1990) and physiological findings (Abeles, 1982a; Eggermont, 1990; Kruger, 1991; Ahissar et al., 1992b; Sakurai, 1993) as appropriate descriptions of neural coding at the network level.

Thus, CCHs should not be interpreted as reflecting particular synaptic networks. Rather, these correlograms should be interpreted as reflecting inter-neuronal information transfer, whose characteristics are crucial for processing at the network level (for a recent review, see Fujii et al. (1996)). For example, functional efficacy describes the ability of one neuron to transfer information to another neuron. With regard to learning rules, this functional level of description is highly relevant.

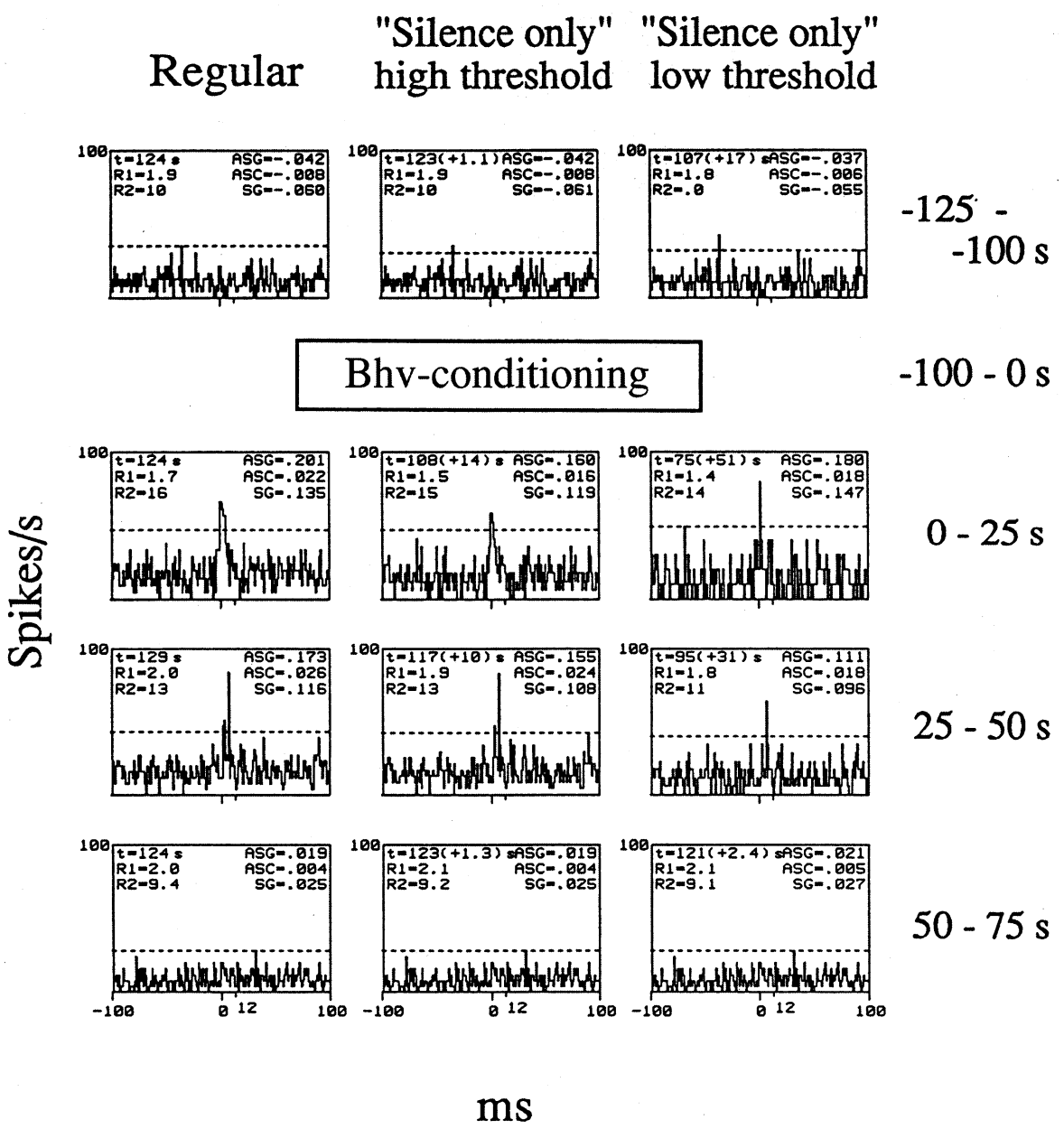

Fig. 12. An example of the effect of the removal of the monkey's SelfGen sounds. SelfGen sections were removed from the data files used to compute Fig. 3 (left CCHs). The process was repeated for the two thresholds that were used to record the SelfGen sound times (middle and right CCHs).

4.2. Significance of functional plasticity

Hebb (1949) described his famous learning rule in functional terms. Undoubtedly, implementations of learning rules depend on intracellular and molecular levels. However, their validity should be tested at the functional, network level. For example, assume that intracellular mechanisms are capable of implementing two different learning rules, say, Hebbian and anti-Hebbian. In this scenario, the questions relevant to behavioral learning are: (i) are the two rules utilized during behavior or only one of them; and (ii) if the two rules apply, do they apply under different behavioral conditions. Measurements of functional plasticity directly probe the level at which such questions should be answered. Thus, the main experimental significance of functional plasticity is in characterizing functional, i.e. activity-related, rules, that underlie learning, and in constraining interpretations of synaptic plasticity.

This study, together with other studies that apply the same approach (Das and Gilbert, 1995), provides a first step in studying functional learning rules in the behaving brain. We showed that functional plasticity requires both changes in functional contingency and a behav-

ioral control. The approach we utilized should also facilitate differentiation between different plausible behavioral factors, such as attention, motivation and reinforcement-driven factors; testing how behavioral control is accomplished in the brain; and determining the relevance of functional plasticity to behavioral learning.

4.3. The functional learning rule in the auditory cortex

As predicted by the covariance (Sejnowski, 1977), Stent's (Stent, 1973), and other (Bienenstock et al., 1982; Brown et al., 1990) rules, and consistent with findings of synaptic plasticity, functional connections could be either potentiated or depressed, depending on the induced correlations. However, functional plasticity in the auditory cortex deviated from the basic covariance rule—functional efficacy was modified according to the change in covariance (see similar suggestions by Fregnac et al. (1988) and Klopf (1989)). That is, strengths of functional couplings remained constant (within the range of spontaneous fluctuations), unless a dramatic change in their coupling was induced. Unlike the covariance rule, this rule is consistent with common observations of steady functional connections (e.g. Shulz et al. (1997)). Also, this rule is in agreement with the 'generalized Hebb rule' suggested by Brown et al. (1990).

One interpretation of the underlying process of functional plasticity is that the average correlation is represented by cellular factors that have time constants of minutes, and are compared against the instantaneous correlation, which is represented with time constants of a few milliseconds. The difference (or ratio) between these two correlation values controls the synaptic modifications:

$$\Delta w = g(\tilde{x}y - \langle \tilde{x}y \rangle) \tag{1}$$

or

$$\Delta w/w = g(\tilde{x}y/\langle \tilde{x}y \rangle) - 1 \tag{2}$$

where Δw is the change in synaptic weight, $\tilde{x}$ denotes a 'trace' of the pre-synaptic activity (Sutton and Barto, 1981) during a few milliseconds (equivalent to the width of the CCH peak), and $\langle a \rangle$ denotes the average over a few minutes of a. Similarly, learning rules can be expressed in terms of covariances instead of correlations, for example:

$$\Delta w/w = g((\tilde{x}y - \langle x \rangle \langle y \rangle)/(\langle \tilde{x}y \rangle - \langle x \rangle \langle y \rangle)) - 1 \tag{3}$$

The control function (g) can be estimated for the divisive covariance rule (Eq. (3)) using the curve fittings in Fig. 8A as:

$$g(z) \approx z^{0.15 + 0.3B} \tag{4}$$

or

$$g(z) \approx (1.1 + 0.8B) z^{0.03 + 0.14B}, \quad z = 2$$

$$g(z) \approx (0.84 - 0.12B) z^{0.2 + 0.05B}, \quad z \leq 0.5 \tag{5}$$

where B stands for the behavioral gating factor ($B = 1$ when the monkey is behaving and 0 otherwise). Note that $\mathrm{SF} = \Delta w/w + 1$ and $\mathrm{CF} = z$.

Our learning functions were expressed as functions of covariance changes, since this is what was measured (Fig. 1). However, these functions could be expressed as functions of correlation changes (Eqs. (1) and (2)), i.e. changes in the total area under the CCH peaks, including the area due to chance correlations. A distinction between correlation and covariance changes, with regard to being the critical parameters in the proposed learning rules, was not addressed in this study. Our suggested rule closely resembles Klopf's rule (Klopf, 1989). If the behavioral control is ignored, these two rules deviate only slightly with regard to the controlling parameter. Klopf's rule relates to the correlation of firing changes, whereas our rule relates to the changes of firing covariances (or, possibly, the changes of firing correlations). Our current data cannot distinguish between Klopf's rule and our's.

Our finding that neuronal plasticity depends on changes of correlations provides another possible solution to the runaway problem, which is inherent in the basic Hebbian and covariance rules (Sutton and Barto, 1981; Sejnowski and Tesauro, 1989; Brown et al., 1990). According to these basic rules, a chance correlation (with Hebb's rule), or a constant covariance due to existing connection (with both Hebb's and the covariance rules), will be continuously strengthened until saturation occurs. Our data suggests the following solution, which can be added to the different solutions previously suggested. When strengthening depends on changes in correlations and when the modification gain is not too high, steady-state finite strengths are possible because of the negative feedback inherent in the learning rule (Ahissar and Ahissar, 1994). This solution to the runaway problem uses the existing correlation strength as a 'balance point' and is somewhat similar to the solution proposed by the 'generalized Hebb rule' (Brown et al., 1990), which uses the existing synaptic strength as a balance point. However, with the monotonically increasing learning rule (thin line in Fig. 8 and Eq. (4)), correlations will tend to oscillate around the steady-state value with periods equivalent to the slow averaging window. In order to avoid such oscillations, learning rules such as the one implied by the thick line in Fig. 8 might be used. In the latter, Hebbian-like modifications (both potentiating and depressing) occur only beyond certain thresholds (e.g. Eq. (5)), and in between those thresholds anti-Hebbian learning occurs. This rule resembles the Bienenstock-Cooper-Munro (BCM) rule (Bienenstock et al., 1982; Fregnac and Shulz, 1994), but with correlation changes instead

of postsynaptic potential as the controlling parameter, and with an extrapolation for $CF < 1$.

4.4. Specificity of functional plasticity

In this study, functional plasticity was specific to those neuronal pairs that fulfilled the requirements of functional learning rules. Potentiations and depressions did not transfer between neuronal pairs that shared one of the conditioned neurons (e.g. Fig. 9). This finding is consistent with mechanisms in which modifications are specific for the involved synapses (Viana Di Prisco, 1984; Fregnac and Shulz, 1994; Cruikshank and Weinberger, 1996b) and not with mechanisms that assume general cellular modifications either in the post-synaptic (Shimbel, 1950) or pre-synaptic (Bonhoeffer et al., 1989) cells.

Specificity of plasticity is often tested using a differential conditioning procedure (Carew et al., 1984). In such paradigms, two CSs, which both have the potential to produce a CR, are used: CS+ and CS−, where CS+ is paired with the US and CS− is delivered randomly. If only the CS+ produces a CR, then the plastic change is considered specific. If both the CS+ and CS− produce a CR, then the plasticity is non-specific. However, this procedure only tests postsynaptic specificity, and not presynaptic specificity. In our study, several single neurons were usually recorded simultaneously, and thus, both specificities could be tested. The procedure we used might be called 'cross-differential conditioning,' since in most of the conditioning sessions there were two CRs in addition to two CSs. For example, in Fig. 9, neurons 4 and 9 can be considered as CS+ and CS−, respectively, and neurons 10 and 9 as CR+ and CR−, respectively. In this typical example, only the CS+ CR+ pair exhibited lasting potentiation.

4.5. Behavioral control of functional plasticity

Contingency changes that were not associated with behavior, on the average, yielded only weak plastic changes. However, when the same contingency changes were associated with behavior in monkey B, much stronger plastic changes were observed. This finding is in agreement with recent findings that link the effectiveness of conditioning to arousal-like EEG states (Cruikshank and Weinberger, 1996a). Potentiations associated with behavior were, when averaged, six times stronger than non-behaving potentiations (increments of 180 versus 30%; Table 3). Intriguingly, this ratio fits Thorndike's estimate that "a single occurrence followed by reward strengthens a connection about six times as much as it would be strengthened by merely occurring" (Thorndike, 1940), and supports Thorndike's "Law of Effect" (Thorndike, 1913). Although a few neuronal pairs in our study exhibited marked plasticity even under the non-behaving condition, all the neuronal pairs recorded under both conditions exhibited stronger changes when the monkey was behaving. The behavioral factors that were differentially engaged in the two behavioral conditions of this study probably included motivation, attention and reinforcement-driven factors. Although we cannot distinguish between the influences of the different behavioral factors based on our experiments, other studies indicate that modality-specific (Recanzone et al., 1993), and task-specific (Ahissar and Hochstein, 1993) attention is probably the major factor that affects cortical plasticity. If this is indeed the case, the limited modifications observed in the non-behaving condition in this study might result from attentional mechanisms that were occasionally activated by the monkey during these periods despite the absence of reward.

Behavioral control of plasticity may be mediated by some (or all) of the ascending diffused systems, and in particular the cholinergic and noradrenergic ones (Crow, 1968; Kety, 1970; Ahissar et al., 1996). These systems could be activated under different behavioral conditions, and consequently act on cortical synapses. Although the involvement of these systems in neuronal plasticity is implied by a variety of experiments (see Ahissar and Ahissar (1994), for a review and a recent study by Kilgard and Merzenich (1998)), the operating mechanisms are far from being understood.

4.6. Elevation of the average firing rate—changes of cellular excitability or reflections of 'memory traces'

In the motor cortex of cats, Woody and colleagues showed that acquisition of classical (behavioral) conditioning is often accompanied by an increase of the general excitability level of single cells (Woody, 1982; Matsumura and Woody, 1986; Aou et al., 1992). However, Baranyi et al. (1991) showed that long-lasting potentiations in awake cats were not correlated with changes in the electrical membrane properties, including spike thresholds, of the same cells. Results similar to Baranyi et al. (1991) were obtained in anaesthetized cats (Baranyi and Feher, 1981a,b,c). Thus, the relevance of excitability changes to learning mechanisms was unclear.

In this study, functional plasticity was often accompanied by an elevation of the average firing rate of the neurons (by about 20% when averaged). This change might occur following an increase in the excitability of the neurons (e.g. a decrease of their firing thresholds), increased pre-synaptic activity, or increased synaptic strengths. Changes in neuronal excitabilities should result in changes of functional efficacies. For example, a functional connection should become stronger if the CR-neuron becomes more excitable, even in the ab-

sence of synaptic changes. If this is so, the observed functional plasticity should be correlated to the excitability changes of the CR-neurons. However, in this study they were not correlated, which indicates that modifications of connectivity strengths are not the outcome of changes of general cellular excitabilities. Such a dissociation between rate changes and correlation changes is also evident with iontophonetic cholinergic application (Shulz et al., 1997). Furthermore, changes in general cellular excitability would have caused non-specific functional plasticity, which was not observed in this study. Thus, we prefer an alternative explanation for the elevation of firing rates of the neurons following successful conditioning: this elevation could reflect a transition to a new 'working point' of the local network, which involves higher firing rates and is caused by the overall strengthening of the connections within that network.

4.7. Conclusions, working hypothesis and future directions

The data obtained from simultaneous extracellular recordings of single cells indicate that the mechanisms underlying neuronal plasticity in the cortex of adult monkeys predominantly obey the essential features of both the 'generalized Hebb rule' and Thorndike's ''Law of Effect''. The results presented suggest a formulation of the generalized Hebb rule in which, as was implied before (Fregnac et al., 1988; Klopf, 1989), modifications depend on changes in correlated activities. Our working hypothesis, thus, is:

> The strength of a neuronal connection is modified as a function of recent changes in the correlation between the activities of the two cells. The modification function is strongly controlled by behavior.

Two possible modification functions are: (i) a monotonic increasing function, and (ii) a monotonic increasing function that operates beyond certain potentiating and depressing thresholds, while a monotonic decreasing function operates in between.

The approach presented here is appropriate for determining: (i) the exact modification function (at the functional level), (ii) the major behavioral factor(s) that participate in the modification function, and (iii) (in association with neuropharmacological methods) how behavioral control is mediated.

Acknowledgements

We wish to thank Amos Arieli, Hagai Bergman, Yizhar Lavner, Eyal Margalit, Benny Carmon, and Israel Nelken for their help during the experiments; Ad Aertsen and Daniel Shulz for helpful discussions; and B. Schick for reviewing the manuscript. This study was supported in part by Grant No. 93-198 from the US-Israel Binational Science Foundation, Jerusalem, Israel.

References

Abeles, M., 1982a. Local Cortical Circuits: an Electrophysiological Study. Springer, Berlin.

Abeles, M., 1982b. Quantification, smoothing, and confidence limits for single-units' histograms. J. Neurosci. Methods 5, 317–325.

Abeles, M., Goldstein, M.H., 1977. Multi-unit train analysis. Proc. IEEE 65, 762–773.

Aertsen, A.M.H.J., Gerstein, G.L., Habib, M.K., Palm, G., 1989. Dynamics of neuronal firing correlation: modulation of 'effective connectivity'. J. Neurophysiol. 61, 900–917.

Aertsen, A., Erb, M., Palm, G., 1994. Dynamics of functional coupling in the cerebral cortex: an attempt at a model-based interpretation. Physica-D 75, 103–128.

Ahissar, E., Ahissar, M., 1994. Plasticity in auditory cortical circuitry. Curr. Opin. Neurobiol. 4, 580–587.

Ahissar, M., Hochstein, S., 1993. Attentional control of early perceptual learning. Proc. Natl. Acad. Sci. USA 90, 5718–5722.

Ahissar, E., Vaadia, E., Ahissar, M., Bergman, H., Arieli, A., Abeles, M., 1992a. Dependence of cortical plasticity on correlated activity of single neurons and on behavioral context. Science 257, 1412–1415.

Ahissar, M., Ahissar, E., Bergman, H., Vaadia, E., 1992b. Encoding of sound source and movement: the activity of single neurons and interactions between adjacent neurons in the primary auditory cortex of monkeys. J. Neurophysiol. 67, 203–215.

Ahissar, E., Haidarliu, S., Shulz, D., 1996. Possible involvement of neuromodulatory systems in cortical Hebbian-like plasticity. J. Physiol. (Paris) 90, 353–360.

Aou, S., Woody, C.D., Birt, D., 1992. Increases in excitability of neurons of the motor cortex of cats after rapid acquisition of eye blink conditioning. J. Neurosci. 12, 560–569.

Artola, A., Brocher, S., Singer, W., 1990. Differential voltage-dependent threshold for inducing long-term depression and long-term potentiation in slices of rat visual cortex. Nature 347, 69–72.

Baranyi, A., Feher, O., 1981a. Selective facilitation of synapses in the neocortex by heterosynaptic facilitation. Brain Res. 212, 164–168.

Baranyi, A., Feher, O., 1981b. Synaptic facilitation requires paired activation of convergent pathways in the neocortex. Nature 290, 413–415.

Baranyi, A., Feher, O., 1981c. Intracellular studies on cortical plasticity: conditioning effect of antidromic activation on test-EPSPs. Exp. Brain Res. 41, 124–134.

Baranyi, A., Szente, M.B., Woody, C.D., 1991. Properties of associative long-lasting potentiation induced by cellular conditioning in the motor cortex of conscious cats. Neuroscience 42, 321–334.

Bedenbaugh, P.H., Gerstein, G.L., Boven, K.H., Aertsen, A.M.H.J., 1988. The meaning of stimulus dependent changes in cross correlation between neuronal spike trains. Soc. Neurosci. Abstr. 14, 651 (Abstract).

Bienenstock, E., Cooper, L.N., Munro, P.W., 1982. Theory for the development of neuron selectivity: orientation specificity and binocular interaction in visual cortex. J. Neurosci. 2, 32–48.

Bonhoeffer, T., Staiger, V., Aertsen, A., 1989. Synaptic plasticity in rat hippocampal slice cultures: local 'Hebbian' conjunction of pre- and postsynaptic stimulation leads to distributed synaptic enhancement. Proc. Natl. Acad. Sci. USA 86, 8113–8117.

Boven, K.H., Aertsen, A., 1990. Dynamics of activity in neuronal networks give rise to fast modulations of functional connectivity.

In: Eckmiller, R., Hartmann, G., Hauske, G., (Eds.), Parallel Processing in Neural Systems and Computers. Elsevier, Amsterdam, p. 53–56.

Brons, J.F., Woody, C.D., 1980. Long-term changes in excitability of cortical neurons after Pavlovian conditioning and extinction. J. Neurophysiol. 44, 605–615.

Brown, T.H., Kairiss, E.W., Keenan, C.L., 1990. Hebbian synapses: biophysical mechanisms and algorithms. Annu. Rev. Neurosci. 13, 475–511.

Byrne, J.H., Berry, W.O., 1989. Neural Models of Plasticity. Academic Press, San Diego, CA.

Carew, T.J., Hawkins, R.D., Abrams, T.W., Kandel, E.R., 1984. A test of Hebb's postulate at identified synapses which mediate classical conditioning in Aplysia. J. Neurosci. 4, 1217–1224.

Cohen, S., 1995. Cholinergic modulations of spontaneous activity, auto- and cross-correlations, and cellular conditioning in the auditory cortex of the anesthetized guinea pig. MSc thesis, The Weizmann Institute, Rehovot, Isreal.

Crow, T.J., 1968. Cortical synapses and reinforcement: a hypothesis. Nature 219, 736–737.

Cruikshank, S.J., Weinberger, N.M., 1996a. Receptive-field plasticity in the adult auditory cortex induced by Hebbian covariance. J. Neurosci. 16, 861–875.

Cruikshank, S.J., Weinberger, N.M., 1996b. Evidence for the Hebbian hypothesis in experience-dependent physiological plasticity of neocortex: a critical review. Brain Res. Brain Res. Rev. 22, 191–228.

Das, A., Gilbert, C.D., 1995. Receptive-field expansion in adult visual-cortex is linked to dynamic changes in strength of cortical connections. J. Neurophysiol. 74, 779–792.

Dickson, J.W., Gerstein, G.L., 1974. Interactions between neurons in auditory cortex of the cat. J. Neurophysiol. 37, 1239–1261.

Edeline, J.M., 1996. Does Hebbian synaptic plasticity explain learning-induced sensory plasticity in adult mammals? J. Physiol. (Paris) 90, 271–276.

Eggermont, J.J., 1990. The Correlative Brain. Theory and Experiment in Neural Interaction. Springer, Berlin.

Fetz, E.E., Gustafson, B., 1983. Relation between shapes of post-synaptic potentials and changes in firing probability of cat motoneuron. J. Physiol. 341, 387–410.

Fregnac, Y., Shulz, D., 1989. Hebbian synapses in the visual cortex. In: Kulikowski, K.K (Ed.), Seeing Contour and Colour. Pergamon, Oxford, p. 711–718.

Fregnac, Y., Shulz, D., 1994. Models of synaptic plasticity and cellular analogs of learning in the developping and adult visual cortex. In: Casagrande, V.A., Shinkman, P.G. (Eds.), Advances in Neural and Behavioral Development, vol. 4. Ablex, New Jersey, p. 149–235.

Fregnac, Y., Shulz, D., Thorpe, S., Bienenstock, E., 1988. A cellular analogue of visual cortical plasticity. Nature 333, 367–370.

Frostig, R.D., Gottlieb, Y., Vaadia, E., Abeles, M., 1983. The effects of stimuli on the activity and functional connectivity of local neuronal groups in the cat auditory cortex. Brain Res. 272, 211–221.

Fujii, H., Ito, H., Aihara, K., Ichinose, N., Tsukada, M., 1996. Dynamical cell assembly hypothesis—theoretical possibility of spatio-temporal coding in the cortex. Neural Netw. 9, 1303–1350.

Gerstein, G.L., Bedenbaugh, P., Aertsen, M.H., 1989. Neuronal assemblies. IEEE. Trans. Biomed. Eng. 36, 4–14.

Hebb, D.O., 1949. The Organization of Behavior. A Neuropsychological Theory. Wiley, New York.

James, W. (1890) The Principles of Psychology. Holt, Reinhart and Winston, New York.

Jones, E.G., Burton, H., 1976. Areal differences in the laminar distribution of thalamic afferents in cortical fields of the insular, parietal and temporal regions of primates. J. Comp. Neurol. 168, 197–248.

Kandel, E.R., Spencer, W.A., 1968. Cellular neurophysiological approaches in the study of learning. Psychol. Rev. 48, 65–134.

Kety, S.S., 1970. The biogenic amines in the central nervous system: their possible roles in arousal, emotion and learning. In: Schmitt, F.O. (Ed.), Neurosciences: Second Study Program. Rockefeller University Press, New York, p. 324–336.

Kilgard, M.P., Merzenich, M.M., 1998. Cortical map reorganization enabled by nucleus basalis activity. Science 279, 1714–1718.

Klopf, A.H., 1989. Classical conditioning phenomena predicted by a drive-reinforcement model of neuronal function. In: Byrne, J.H., Berry, W.O. (Eds.), Neural Models of Plasticity. Academic Press, San Diego, CA, p. 104–132.

Kruger, J. (Ed.), 1991. Neuronal Cooperativity. Springer, Berlin.

Levick, W.R., Cleland, B.G., Dubin, M.W., 1972. Lateral geniculate neurons of cat: retinal inputs and physiology. Invest. Ophthalmol. 11, 302–311.

Levy, W.B., 1989. A computational approach to hippocampal function. In: Hawkins, R.D., Bower, G.H. (Eds.), Computational Models of Learning in Simple Neural Systems. Academic Press, New York, p. 243–305.

Markram, H., Tsodyks, M., 1996. Redistribution of synaptic efficacy between neocortical pyramidal neurons. Nature 382, 807–810.

Matsumura, M., Woody, C.D., 1986. Long-term increases in excitability of facial motoneurons and other neurons in and near the facial nuclei after presentations of stimuli leading to acquisition of a Pavlovian conditioned facial movement. Neurosci. Res. 3, 568–589.

Merzenich, M.M., Recanzone, G.H., Jenkins, W.M., Grajski, K.A., 1990. Adaptive mechanisms in cortical networks underlying cortical contributions to learning and nondeclarative memory. Cold Springs Harbor Symp. Quant. Biol. 55, 873–887.

Moore, G.P., Segundo, J.P., Perkel, D.H., Levitan, H., 1970. Statistical signs of synaptic interactions in neurons. Biophys. J. 10, 876–900.

Perkel, D.H., Gerstein, G.L., Moore, G.P., 1967. Neuronal spike trains and stochastic processes. II. Simultaneous spike trains. Biophys. J. 7, 419–440.

Pfingst, B.E., O'Connor, T.A., 1980. A vertical stereotaxic approach to auditory cortex in the unanesthetized monkey. J. Neurosci. Methods 2, 33–45.

Pons, T.P., Garraghty, P.E., Ommaya, A.K., Kaas, J.H., Taub, E., Mishkin, M., 1991. Massive cortical reorganization after sensory deafferentation in adult macaques. Science 252, 1857–1860.

Rauschecker, J.P., 1991. Mechanisms of visual plasticity: Hebb synapses, NMDA receptors, and beyond. Physiol. Rev. 71, 587–615.

Recanzone, G.H., Schreiner, C.E., Merzenich, M.M., 1993. Plasticity in the frequency representation of primary auditory cortex following discrimination training in adult owl monkeys. J. Neurosci. 13, 87–103.

Sakurai, Y., 1993. Dependence of functional synaptic connections of hippocampal and neocortical neurons on types of memory. Neurosci. Lett. 158, 181–184.

Sanides, F., 1972. Representation in the cerebral cortex and its lamination pattern. In: Bourne, G.H. (Ed.), The Structure and Function of Nervous Tissue. Academic Press, New York, p. 329–453.

Sejnowski, T.J., 1977. Storing covariance with nonlinearly interacting neurons. J. Math. Biol. 4, 303–321.

Sejnowski, T.J. and Tesauro, G.J. (1989) The Hebb rule for synaptic plasticity: implementations and applications. In: Byrne, J.H., Berry, W.O. (Eds.), Neural Models of Plasticity. Academic Press, San Diego, CA, p. 94–103.

Shimbel, A., 1950. Contribution to the mathematical biophysics of the central nervous system with special reference to learning. Bull. Math. Biophys. 12, 241–275.

Shulz, D., Debanne, D., Fregnac, Y., 1993. Cortical convergence of ON- and OFF-pathways and functional adaptation of receptive field organization in cat area 17. Prog. Brain Res. 95, 191–205.

Shulz, D., Cohen, S., Haidarliu, S., Ahissar, E., 1997. Differential effects of acetylcholine on neuronal activity and interactions in the auditory cortex of the guinea pig. Eur. J. Neurosci. 9, 396–409.

Stent, G.S., 1973. A physiological mechanism for Hebb's postulate of learning. Proc. Natl. Acad. Sci. USA 70, 997–1001.

Sutton, R.S., Barto, A.G., 1981. Toward a modern theory of adaptive networks: expectation and prediction. Psychol. Rev. 88, 135–170.

Thorndike, E.L., 1913. The Psychology of Learning. (Educational Psychology II). Teachers College, New York.

Thorndike, E.L., 1940. Human Nature and the Social Order. Macmillan, New York, p. 14.

Uttley, A.M. (1976) Information Transmission in the Nervous System. Academic Press, London.

Vaadia, E., Ahissar, E., Bergman, H., Lavner, Y., 1991. Correlated activity of neurons: a neural code for higher brain functions? In: Kruger, J. (Ed.), Neuronal Cooperativity. Springer, Berlin, p. 249–279.

Vaadia, E., Haalman, I., Abeles, M., et al., 1995. Dynamics of neuronal interactions in monkey cortex in relation to behavioural events. Nature 373, 515–518.

Viana Di Prisco, G., 1984. Hebb synaptic plasticity. Prog. Neurobiol. 22, 89–102.

Weinberger, N.M., 1993. Learning-induced changes of auditory receptive fields. Curr. Opin. Neurobiol. 3, 570–577.

Weinberger, N.M., 1995. Dynamic regulation of receptive fields and maps in the adult sensory cortex. Annu. Rev. Neurosci. 18, 129–158.

Woody, C.D., 1982. Acquisition of conditioned facial reflexes in the cat: cortical control of different facial movements. Fed. Proc. 41, 2160–2168.